

A STUDY OF INTERACTION EFFECTS DUE TO BORED TUNNELS IN CLAY

by

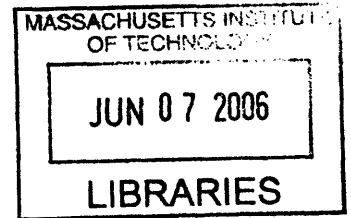
Paul Sweeney

B.A.I. Civil Engineering
University of Dublin, Trinity College

Submitted to the department of
Civil and Environmental Engineering in
Partial Fulfillment of the Requirements for the Degree of

Master in Engineering in
Civil and Environmental Engineering
at the
Massachusetts Institute of Technology

June 2006



© 2006 Paul Sweeney. All rights reserved

The author hereby grants to MIT permission to reproduce and to distribute publicly paper and electronic copies of this thesis document in whole or in part in any medium now known or hereafter created.

BARKER

Signature of Author: _____
Department of Civil and Environmental Engineering
May 26, 2006

Certified by: _____
Andrew Whittle
Professor of Civil and Environmental Engineering
Thesis Supervisor

Accepted by: _____
Andrew Whittle
Professor of Civil and Environmental Engineering
Chairman, Departmental Committee for Graduate Students

A STUDY OF INTERACTION EFFECTS DUE TO BORED TUNNELS IN CLAY

by

Paul Sweeney

Submitted to the Department of Civil and
Environmental Engineering on May 26, 2006 in
Partial Fulfillment of the Degree Requirements for
Master of Engineering in Civil and Environmental Engineering

ABSTRACT

As more and more tunnels are being bored in urban environments it is essential to understand the effects that this will have on adjacent structures, for example, the state of Singapore, which has been expanding its underground transit system extensively. The effects of tunneling twin tunnels in Singapore marine clay are outlined, analyzed and discussed. Three different configurations are taken into account, side-by-side tunnels, piggyback tunnels and angular-offset tunnels, located at a typical depth for Singapore. Empirical correlations, derived from extensive field data, are used to calculate ground movements caused by twin bored tunnel constructions using superposition. Non-linear finite element analysis is used for the same situations, as well as for analyzing the stresses in the tunnel lining. The use of superposition was tested using the non-linear analysis to check whether or not its use with empirical methods is appropriate. Although the numerical solutions suggest that superposition is a good approximation for twin tunnel bores, there is a clear discrepancy in the magnitude and distribution of ground movements calculated by empirical and numerical solutions.

Thesis Supervisor: Andrew Whittle
Title: Professor of Civil and Environmental Engineering

ACKNOWLEDGEMENTS

I would like to thank my family for their continuing support, Professor Whittle for his expert guidance, the MFISH team for humor in the face of adversity, the rest of the M.Eng class for humor without adversity, and finally, my girlfriend Sinéad for putting up with all my flip.

TABLE OF CONTENTS

ACKNOWLEDGMENTS.....	3
TABLE OF CONTENTS.....	4
LIST OF FIGURES.....	5
LIST OF TABLES.....	7
1.0 INTRODUCTION.....	8
2.0 TUNNEL CONSTRUCTION.....	9
3.0 EMPIRICAL METHODS.....	11
3.1 SINGLE TUNNEL.....	11
3.1.1 SURFACE EFFECTS	11
3.1.2 SUBSURFACE EFFECTS	13
3.2 TWIN TUNNELS.....	18
3.2.1 SURFACE EFFECTS	20
3.2.2 SUBSURFACE EFFECTS	27
4.0 FINITE ELEMENT ANALYSISOF TWIN TUNNELS.....	31
4.1 GROUND MOVEMENTS.....	31
4.1.1 SURFACE EFFECTS	33
4.1.2 SUBSURFACE EFFECTS	39
4.2 LINING STRESSES.....	44
4.2.1 SIDE-BY-SIDE TUNNELS	45
4.2.2 PIGGYBACK TUNNELS	48
4.2.3 ANGULAR-OFFSET TUNNELS	50
5.0 COMPARISON OF NUMERICAL AND EMPIRICAL METHODS.....	52
5.1 COMPARISON OF GROUND MOVEMENTS.....	52
5.1.1 SIDE-BY-SIDE TUNNELS	52
5.1.2 PIGGYBACK TUNNELS	55
5.1.3 ANGULAR-OFFSET TUNNELS	56
6.0 CONCLUSIONS	58
REFERENCES.....	59

LIST OF FIGURES

Page

Figure 1 – Surface settlement troughs from various empirical methods	13
Figure 2 – Subsurface settlement troughs from various empirical methods	15
Figure 3 – Settlement profile with depth	16
Figure 4 – Lateral deflections from tunnel construction	17
Figure 5 – Various types of twin tunnel construction	18
Figure 6 – Effect of distance between side-by-side tunnels on S_{max}	20
Figure 7 – Empirical settlement trough for twin bored tunnels ($X_t = 15m$)	21
Figure 8 – Empirical settlement trough for twin bored tunnels ($X_t = 35m$)	22
Figure 9 – Effect of distance between piggyback tunnels on S_{max}	23
Figure 10 – Empirical settlement trough for twin piggyback tunnels	24
Figure 11 – Effect of distance between angular tunnels on S_{max}	25
Figure 12 – Empirical settlement trough for angular tunnel (45°)	26
Figure 13 – Lateral Movements with depth for side-by-side tunnels	27
Figure 14 – Lateral movements estimated between side-by-side tunnels	28
Figure 15 – Lateral deformations for piggyback tunnels ($x=10m$)	29
Figure 16 – Lateral deformations for angular tunnels	30
Figure 17 – Soil Properties with depth	32
Figure 18 - Effect of distance between tunnels on S_{max}	33
Figure 19 – FE settlement troughs for side-by-side tunnels ($X_t = 15m$)	34
Figure 20 – FE settlement troughs for side-by-side tunnels ($X_t = 35m$)	34
Figure 21 – FE Settlement troughs for piggyback tunnels ($X_t = 15m$)	35
Figure 22 – Effect of distance between angular tunnels on S_{max}	37
Figure 23 – FE settlement troughs for Angular Tunnels ($X_t=15m$)	38
Figure 24 – FE Lateral movements with depth for side-by-side tunnels	39
Figure 25 – FE Lateral movements estimated between lateral tunnels	40
Figure 26 – FE Lateral deformations for piggyback tunnels ($x = 10m$)	41
Figure 27 – FE Lateral deformations for angular tunnels	42
Figure 28 – Plastic Zone Surround Side-By-Side Tunnels	43
Figure 29 – Effect of distance on bending moments in side-by-side tunnels	45

Figure 30 – Bending Moment in first tunnel only	46
Figure 31 – Bending moment in first due to second	46
Figure 32 – Bending moment in second tunnel	47
Figure 33 – Effect of distance on bending moments in piggyback tunnels	48
Figure 34 – Effect of distance on bending moments in piggyback tunnels	49
Figure 35 – Effect of distance on bending moments in angular-offset tunnels	50
Figure 36 – Effect of distance on bending moments in angular-offset tunnels	51
Figure 37 – FE vs. Empirical surface settlement for side-by-side tunnels	52
Figure 38 – FE vs. Empirical lateral movements for side-by-side tunnels	53
Figure 39 – FE vs. Empirical lateral movements between side-by-side tunnels	54
Figure 40 – FE vs. Empirical surface settlement troughs for piggyback tunnels	55
Figure 41 – FE vs. Empirical lateral movements for piggyback tunnels	55
Figure 42 – FE vs. Empirical surface settlement troughs for angular-offset tunnels	56
Figure 43 – FE vs. Empirical lateral movements for angular-offset tunnels	57

LIST OF TABLES

Page

Table 1 – Inflection dimension proposed by various researchers

10

Table 2 – Properties of Singapore marine clay

31

Table 3 – Properties of tunnel lining

31

1.0 INTRODUCTION

Tunnel construction inevitably causes movements in the surrounding soil. This is an important factor during the design phase and the selection of the appropriate method of construction, especially in urban environments, where there are numerous subsurface structures, including foundations, basements and other pre-existing tunnels. Therefore, the alignment of the new tunnel must be carefully chosen to minimize the negative effects caused by ground movement. Apart from the existing structures, there may also be unwanted effects during construction of twin tunnels (commonly selected in transit projects). Although this situation is easier to control, there is little information on the interactions between twin tunnel bores and their combined effects on surface and subsurface ground movements.

The objective of this thesis is to examine the interaction effects caused by construction of twin tunnels bored in clay. There are two methods for analyzing the ground movements surrounding bored tunnels:

- Empirical Correlations
- Numerical Methods (mainly non-linear, finite element methods)

The thesis gives an overview of these methods and then presents results of analyses using Singapore Marine Clay (MFISH, 2006). The analysis will examine the surface and subsurface movements as well as the stresses in the tunnel lining, for different configurations of twin tunnels, side-by-side, piggyback and relative angular-offset.

2.0 TUNNEL CONSTRUCTION

When planning a tunnel one of the more important decisions to be made involves the choice of construction method to be used. In soft clay, such as the Singapore marine clay used in later analyses, it is important to use a closed-face shield with controlled earth pressures to ensure stability of the tunnel face and minimize ground movements.

In practice, there are two types of closed-face shield tunnel boring machines that can be used in unstable soft ground conditions. 1) Earth Pressure Balance (EPB) shields use the excavated soil with additives within a pressurized chamber at the face. The face pressure is controlled by the rate of advance and the speed of the screw conveyor, which is used to remove the soil from the face. 2) Slurry support shields use pressurized bentonite slurry at the cutting face to create a near impermeable layer, which seals the face. This can be used in nearly all soil conditions but is best used in more permeable sandy soils. The EPB is the most suitable shield method for the soil conditions assumed in this thesis, (a deep clay layer beneath the water table).

One of the key parameters in calculating the ground loss is the *volume loss parameter* (V_L). This is defined as the ratio of the volume of the observed settlement trough to the volume occupied by the tunnel lining. Volume losses occur due to a variety of factors including overrating of the minimal tunnel diameter (tail void), methodology of grouting, control of face pressures, local ground conditions etc. It is generally expressed as:

$$V_L = \frac{V_s}{V_t} \quad (1)$$

Where:
 V_L = Volume loss parameter (%)
 V_s = Volume of surface settlement trough
 V_t = Volume occupied by the tunnel

In practice V_L is usually quantified by empirical methods. For EPB tunnel construction in soft clay the volume loss parameter is often linked to the face stability parameter (Mair & Taylor, 1997)

$$N = \frac{\sigma_v - \sigma_t}{Su} \quad (2)$$

Where, σ_v is the overburden pressure, σ_t is the pressure inside the tunnel face and Su is the undrained shear strength. For bored tunnels in Singapore the springline is typically located at $Z = 20-35\text{m}$ such that $\sigma_v = 350-600\text{kPa}$, $Su = 30-50\text{kPa}$, hence the stability of the face and the volume loss depends on the face pressure, σ_t . For a deep clay situation typical values of V_L are 1-2%. The analyses in this thesis assume a constant value, $V_L = 2\%$.

3.0 EMPIRICAL METHODS

These methods, derived from observed field measurements, are well-established and are primarily used for estimating surface settlement, though there are some results available for calculating subsurface movements. The following section will outline the empirical methods available for a single tunnel, twin tunnels, for both surface and subsurface ground movements.

3.1 SINGLE TUNNEL

Before the effects caused by twin tunnels are investigated it is important to understand the effects of a single tunnel. Once this is done, the effects of two tunnels can be calculated using the principle of superposition for surface settlement by analyzing bending moments caused by the subsurface movements of one tunnel on another.

3.1.1 SURFACE EFFECTS

The most commonly used empirical method is that put forward by Schmidt (1966) who, proposed that the settlement trough could be represented by a Gaussian distribution curve (Figure 1).

$$S = S_{\max} \cdot \exp\left(\frac{-x^2}{2i^2}\right) \quad (3)$$

Where: S= surface settlement at distance x from tunnel centerline
 S_{\max} = maximum settlement at x=0
 x = distance from tunnel centre line
 i = the location of point of inflexion

Here, S_{\max} can be calculated using the following equation:

$$S_{\max} = \frac{0.313V_L D^2}{i} \quad (4)$$

Where: D is the diameter of the tunnel, and i is the lateral distance to the point of inflection in the settlement trough.

Table 1: Inflection dimension proposed by various researchers

Name	i-value	Additional Comments
Peck (1969)	$\frac{i}{R} = \left(\frac{Z_0}{2R}\right)^n$	n = 0.8 to 1.0
Atkinson & Potts (1979)	$i = 0.25(Z_0 + R)$:loose sand $i = 0.25(1.5Z_0 + 0.5R)$:dense sand and over consolidated clay	-
O'Reilly & New (1982)	$i = 0.43Z_0 + 1.1$:Cohesive Soil $i = 0.28Z_0 - 0.1$:Granular Soil	-
Mair (1983)	$i = 0.5Z_0$	-
Attewell et al (1977)	$\frac{i}{R} = \alpha \cdot \left(\frac{Z_0}{2R}\right)^n$	$\alpha = 1$ and $n = 1$
Clough & Schmidt (1981)	$\frac{i}{R} = \alpha \cdot \left(\frac{Z_0}{2R}\right)^n$	$\alpha = 1$ and $n = 0.8$

Where: Z_0 = Depth of the tunnel springline below ground surface
R = Tunnel Radius

Using this table, equations 3 and 4 and assuming constant values for R, Z_0 and V_L the different i-values can be directly compared. For this the following values are assumed, and resulting surface settlement trough plotted in Figure 1.

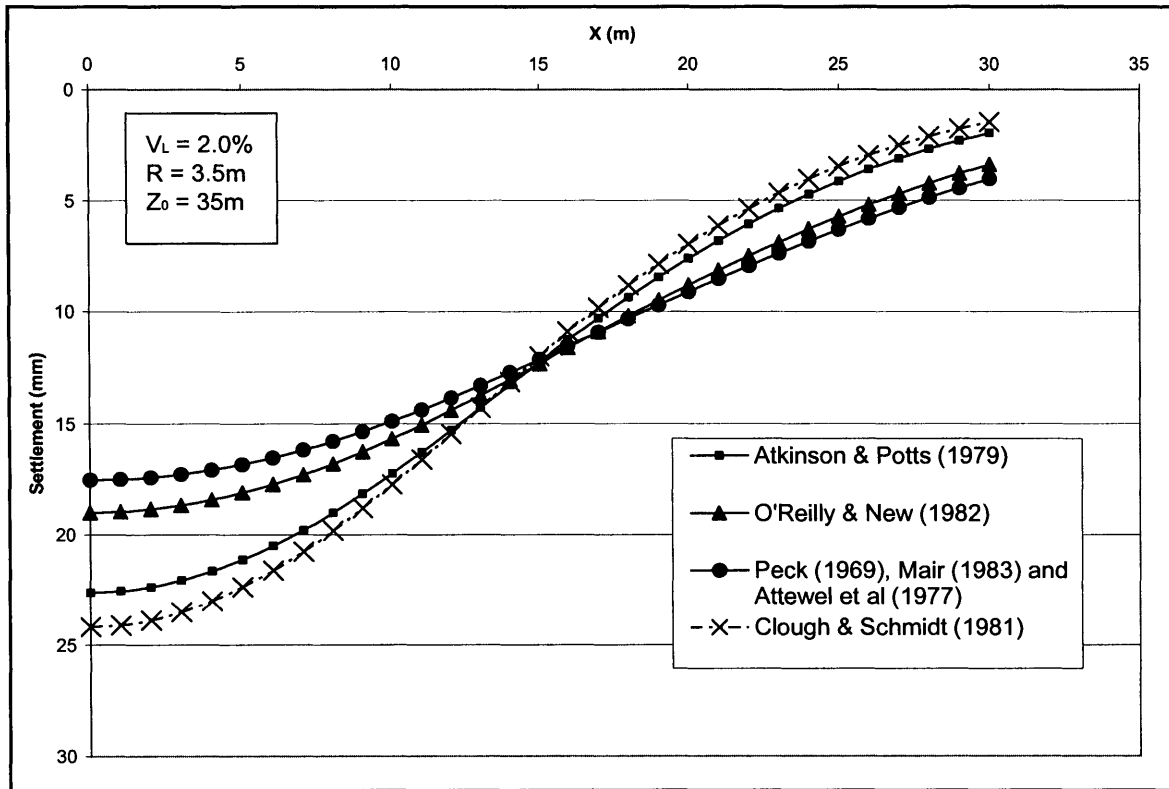


Figure 1. Surface settlement troughs from various empirical methods.

The values of S_{max} range from 17mm to 24mm and the location of the point of inflexion ranges from 13.5m to 17.5m.

3.1.2 SUBSURFACE EFFECTS

Compared to surface settlement methods, there are few empirical methods to predict the subsurface settlements and even fewer to predict lateral deformations. It is often assumed that the subsurface settlement profiles developed during tunnel construction are also characterized by a Gaussian distribution (Mair, 1993). Three of the most widely-used methods are: Mair (1993), Atkinson & Potts (1979) and Vermeer et al. (1991).

Mair (1993) proposed the following method:

$$S_z = S_{z,\max} \exp\left(\frac{-x^2}{2i_z^2}\right) \quad (5)$$

Where: $i_z = k(Z_0 - Z)$ (6)

$$k = \frac{0.175 + 0.325\left(1 - \frac{Z}{Z_0}\right)}{1 - \frac{Z}{Z_0}} \quad (7)$$

$$S_{z,\max} = \frac{1.25V_L}{0.175 + 0.325\left(1 - \frac{Z}{Z_0}\right)} \cdot \frac{R^2}{Z_0} \quad (8)$$

and, $S_{z,\max}$ = maximum settlement at depth, z, S_z = Settlement at depth, z at distance x from centerline

These equations can be used to find the settlement trough at any depth and can also be used to find the settlement profile at any distance from the tunnel centerline.

Atkinson & Potts (1979) proposed the following method:

$$S_z = S_{z,\max} \left\{ 1.0 - \alpha \left(\frac{Z - R}{2R} \right) \right\} \cdot \exp\left(\frac{-x^2}{2i_z^2}\right) \quad (9)$$

Where: $\alpha = 0.57$ for dense sand
 $\alpha = 0.40$ for loose sand
 $\alpha = 0.13$ for over consolidated clay

The final empirical method for estimating subsurface settlement was proposed by Vermeer et al (1991):

$$S_z = \left(\frac{Z_0}{Z_0 - R} \right)^{0.8} S_{z,\max} \exp\left(\frac{-x^2}{2i_z} \right) \tag{10}$$

In order to compare these three methods, two comparisons are required, one for a constant Z and one for a constant x which can be seen in Figures 2 and 3 respectively.

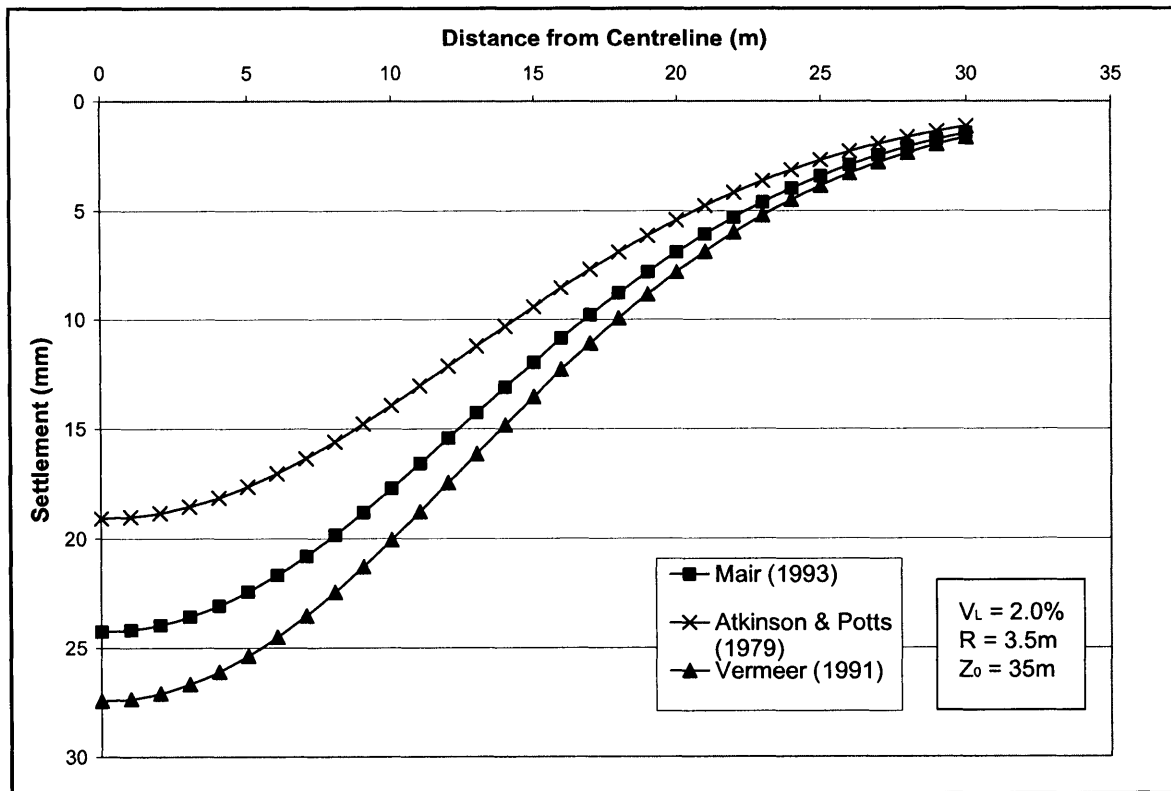


Figure 2. Subsurface settlement troughs from various empirical methods ($Z/Z_0=0.5$).

As with the surface troughs it can be seen that there is some variability in these methods as the settlement values vary by about 9mm. However, all the methods are based on a single i_z value so the farther from the centre line the estimates are taken the closer the results from each method become.

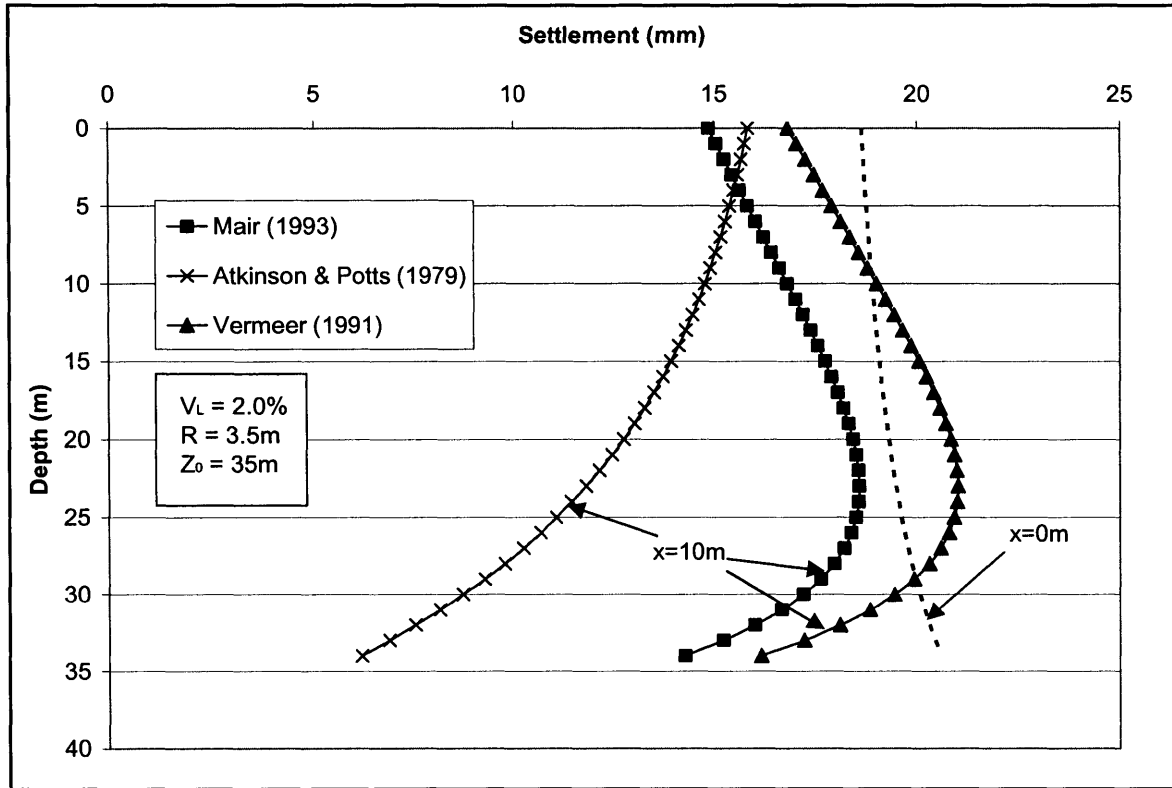


Figure 3. Settlement profile with depth ($X/Z_0=0.35$).

It can be seen from Figure 3 that the maximum settlement that occurs in the soil occurs within about 10m above the tunnel centre line. The closer to the tunnel centerline the estimates are made, the nearer the maximum estimated settlement gets to the tunnel lining, which is indicated by the line ($x = 0$) in Figure 3.

The final part of the empirical section is the estimation of the lateral movements in the soil. There has been very little research into this matter, however there is one empirical method which was proposed by Attewell et al. (1986).

$$S_x = \frac{x}{Z_0} S_z \tag{11}$$

Where: S_x = Lateral deflection

The lateral deflection is a function of the vertical settlement at a depth Z , and a distance x from the centerline. Using the values for S_z from the previous methods Figure 4 is plotted.

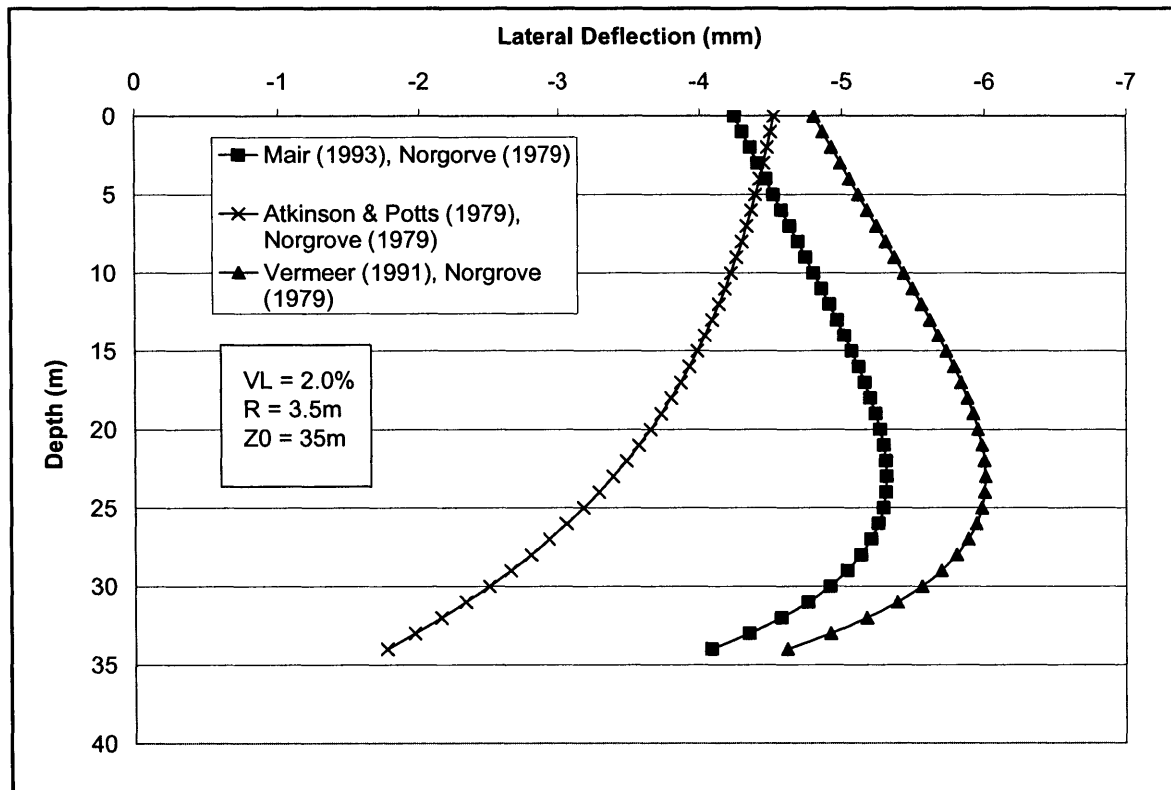


Figure 4. Lateral deflections from tunnel construction ($X/Z_0 = 0.35$).

This estimation doesn't take into account the volume loss that would be caused by lateral deformation, as it takes a value of V_L based only on the volume lost due to vertical settlement. However, it does give a good indication of the profile of lateral deflection that can be expected when constructing a tunnel in clay.

3.2 TWIN TUNNELS

Now that the ground movements associated with a single tunnel have been outlined, the effects of twin tunnel construction can be analyzed. Using empirical calculations three tunnel configurations are considered in this thesis; side by side, piggyback and angular-offset (Figure 5). Common practice is to superimpose the independent settlements estimated for each tunnel to get the final settlement profile. This method is useful for analyzing tunnels which have different radii, different depths and different amounts of ground loss.

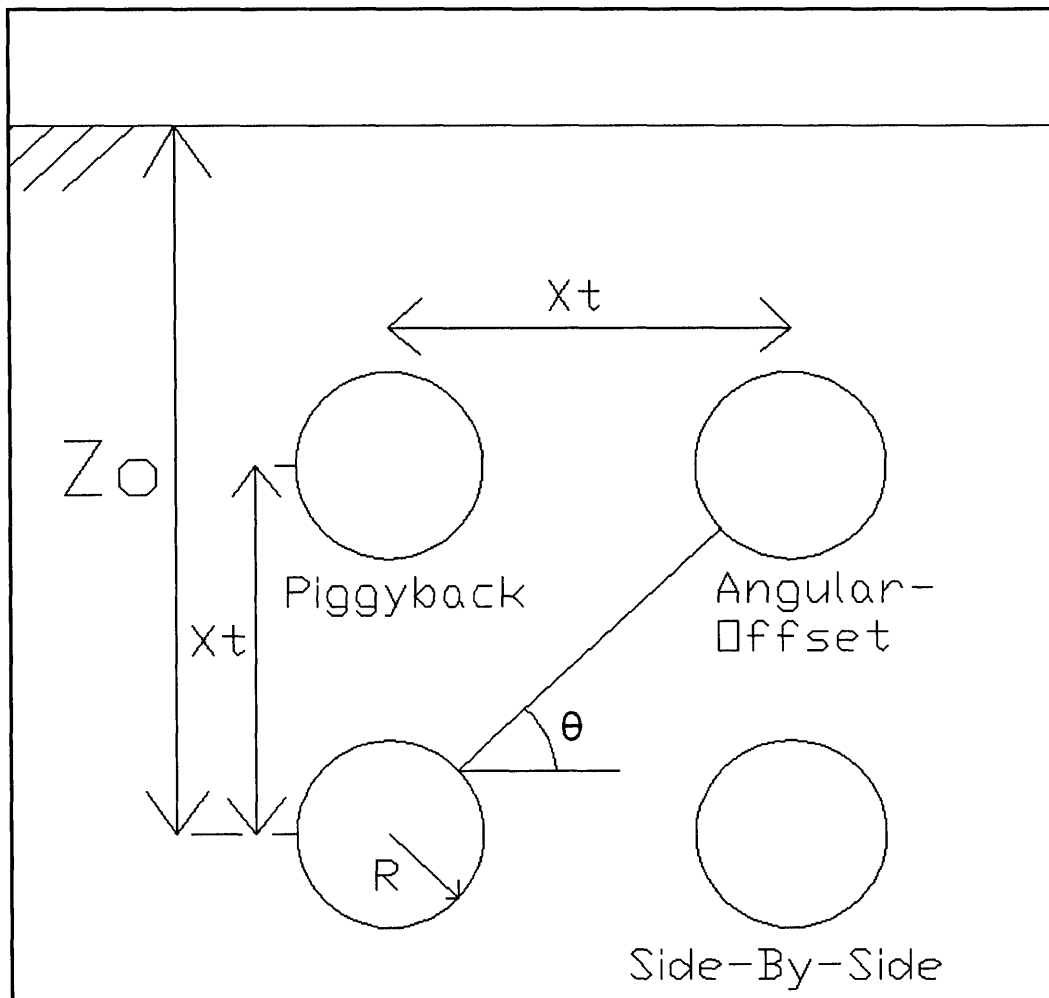


Figure 5. Various configurations of twin tunnel construction.

While this is very useful for quick analysis of the effects of twin tunnels it does not take into account many aspects of tunnel construction which could have a significant effect on the magnitude of settlement, such as:

- Length of time between driving tunnels
- Consolidation movement
- Assumes first tunnel has no effect on ground displacements caused by second tunnel

For the comparison of the effects of twin tunnel construction the distance and position of the tunnels will be varied, while the same values used for the comparison of the single tunnel ground movement will be used. This will be done for a side-by-side tunnel, a piggyback tunnel and a tunnel at a relative angular position of 45° , each at a distance of 15m.

3.2.1 SURFACE EFFECTS

Assuming that both tunnels are 7m diameter bored tunnels with $V_L = 2\%$. The in-place tunnel is at 35m depth, the side-by-side tunnels are at the same depth while the piggyback and angular-offset configurations

Side-by-Side Tunnels

Using the equation 3 and the assumptions above, the settlement profile of these tunnels were calculated for varying distances from centerline to centerline. The maximum settlement for each is shown in Figure 6 the distance between tunnel centerlines, X_t , varies from 15m to 100m.

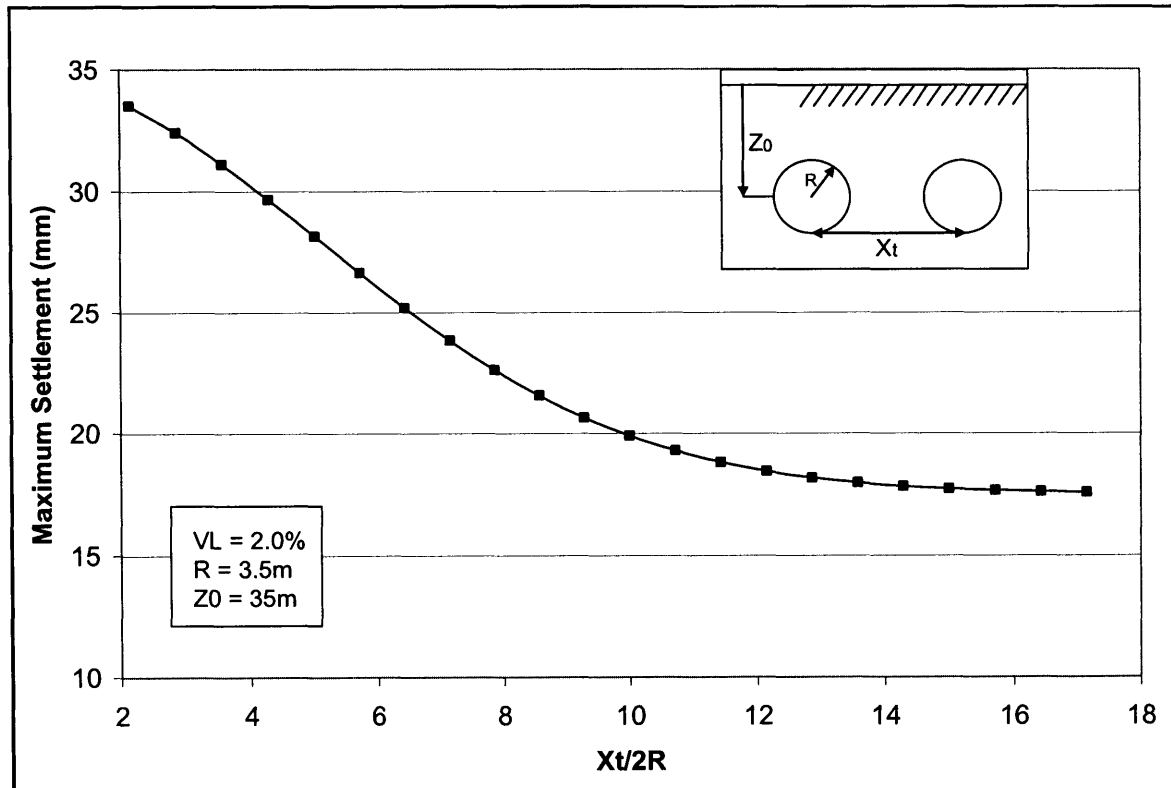


Figure 6. Effect of distance between side-by-side tunnels on S_{max} using empirical methods with superposition (Equation 3).

From this diagram it can be seen that the farther away that the tunnels are constructed from each other, the lesser the maximum settlement on the surface. And at a certain distance relative to the tunnel diameter there will be no significant interaction effects.

Settlement increases as the tunnels get closer due to the combined effect of the volume loss parameters. In general practice, tunnels will not be built within 2 diameters of each other's center line. In figure 7, the settlement profile can be seen for $X_t \approx 4R$. The effect of the second tunnel clearly creates a much deeper trough (32mm as opposed to 18mm).

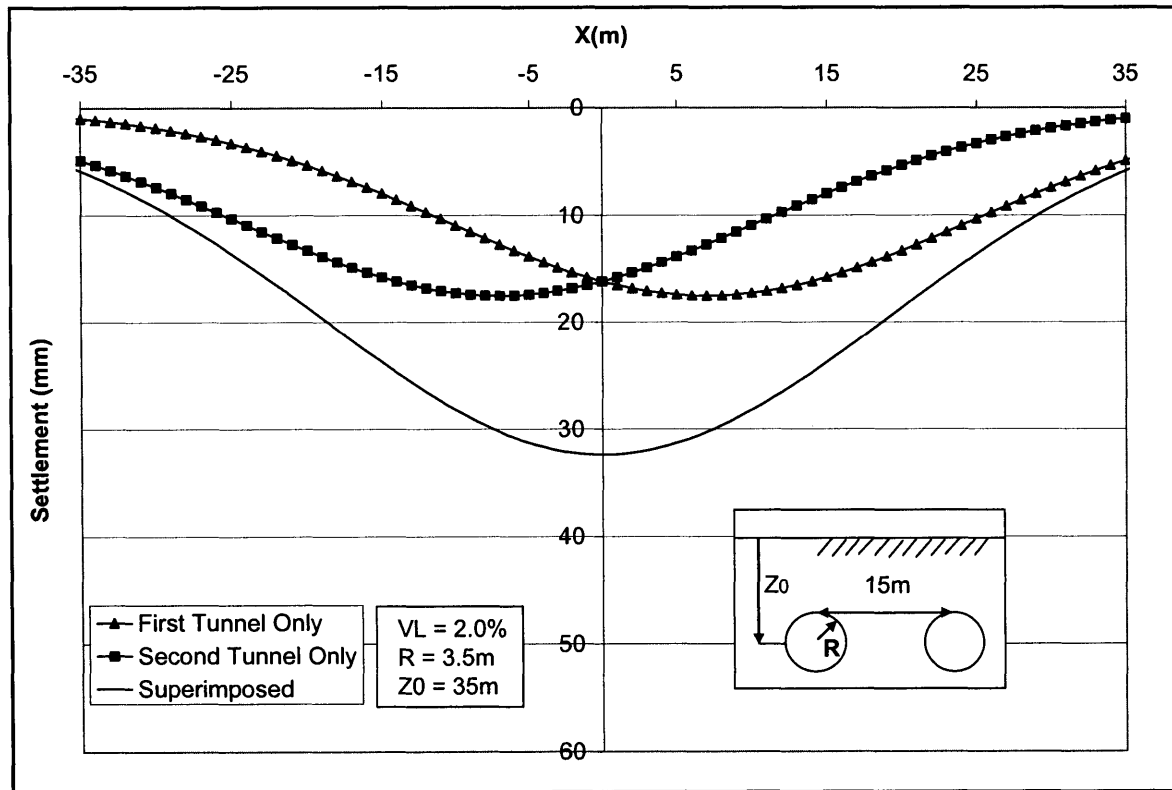


Figure 7. Empirical settlement trough for side-by-side tunnels at $X_t/R = 4$ by superposition of empirical equations (Equation 3).

The increased gradient on the surface can cause difficulties if building in a sensitive area, such as beneath an urban area so therefore this analysis of the settlement could be used to find the optimum distance between the tunnels in order to optimize cost vs. risk.

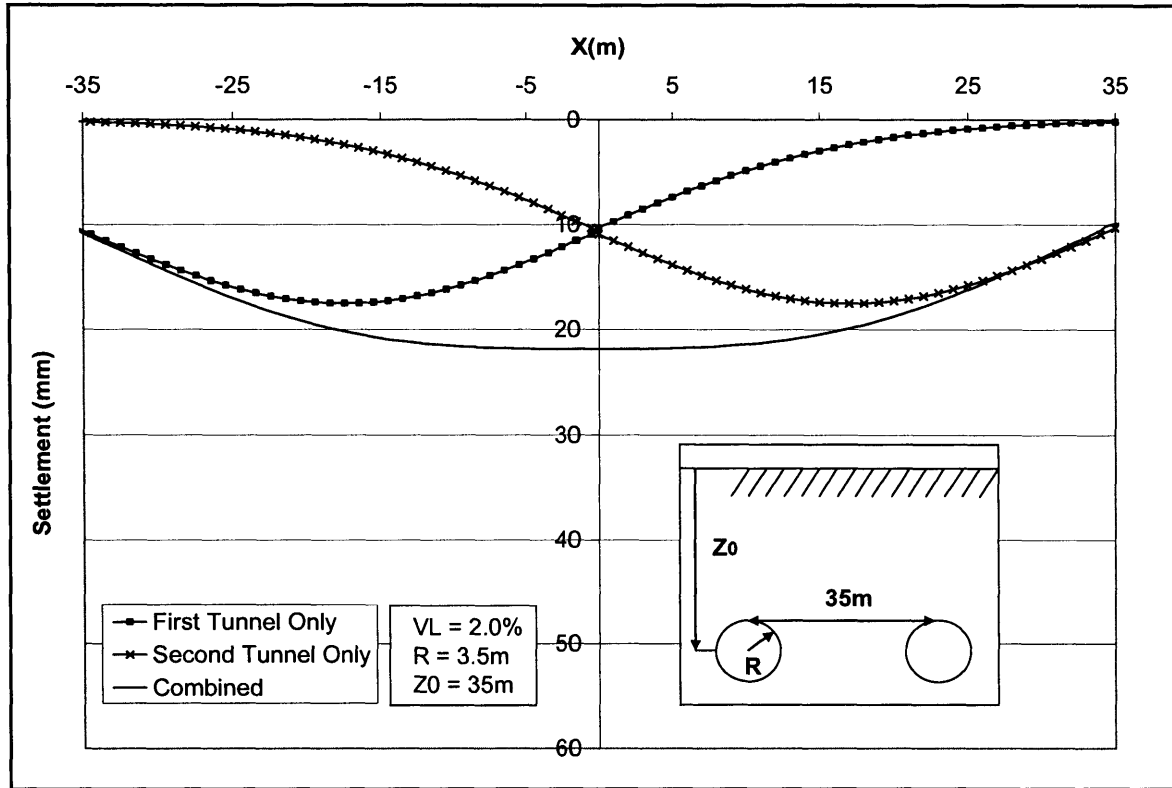


Figure 8. Empirical settlement trough for side-by-side tunnels at $X_t/Z = 1$ by superposition of empirical equations (Equation 3).

In Figure 8, the tunnels are spaced at $X_t/R = 10$ from centerline to centerline and the difference from Figure 7 can clearly be seen. The maximum settlement is being reduced to 23mm and it is settling more evenly at the surface between the tunnels. The surface gradient is almost identical to a single tunnel so there is no increased risk of damage from building one tunnel. So according to this empirical method, the negative interaction effects are reduced significantly. The other interaction effect to be considered is the bending moment that is induced in the existing tunnel. These are discussed and analyzed in chapter 4.

Piggyback Tunnels

The interaction of the piggyback configuration introduces a new issue relating to the order of construction. For side-by-side tunnels it is assumed that there is no difference if one is built before the other. However, with piggyback tunnels there can be an increased interaction as a result of constructing one tunnel above or below the other. This is not considered in the empirical analyses which are based on superposition, but can be considered using numerical analyses, chapter 4. In Figure 9, the effect that the distance between the two tunnels has on the maximum settlement can be seen.

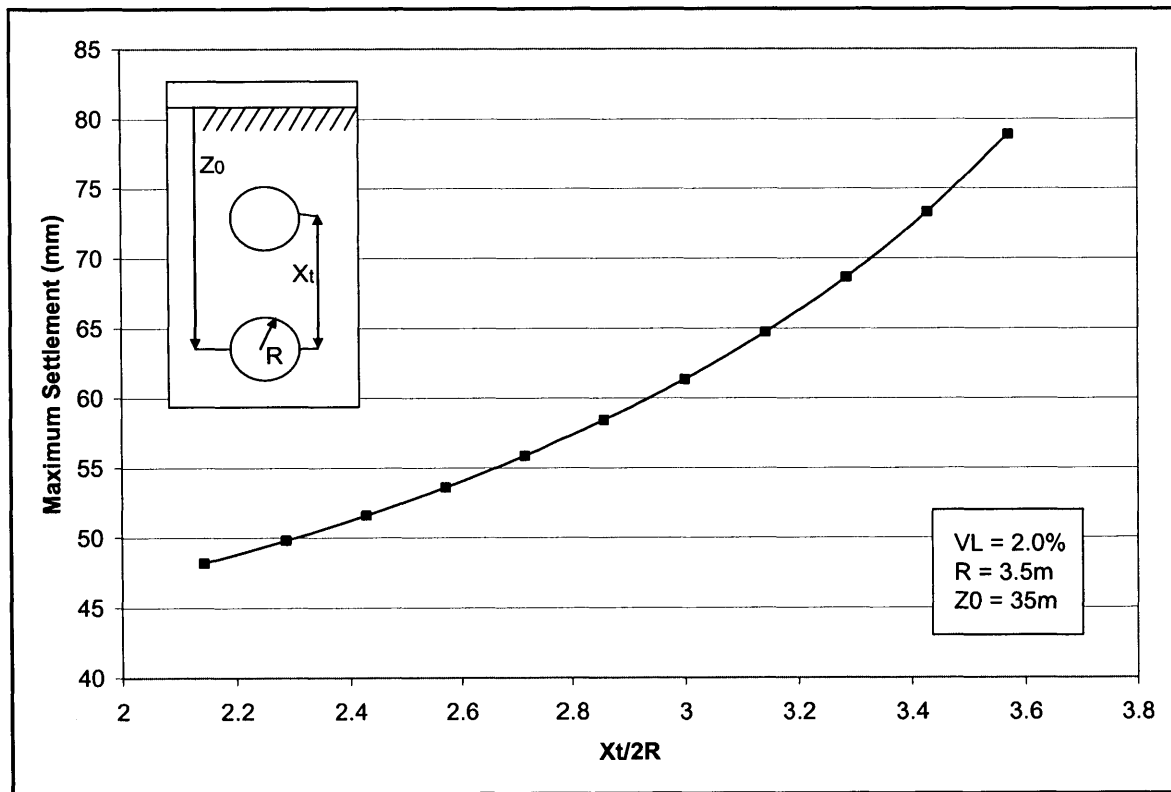


Figure 9. Effect of distance between piggy back tunnels on S_{max} based on superposition of empirical solutions (Equation 3)

In the analysis for Figure 9, the first tunnel was taken to be the same as previous examples and the upper tunnel's location varied from 20m to 10m. As can be seen from Figure 9, the closer the tunnel is constructed to the surface the larger the maximum settlement is estimated to be. This is due to the subsurface settlements increasing as measurements are taken nearer to the tunnel. An empirical piggyback trough can be seen in Figure 10 for tunnels at 35m and 20m depth.

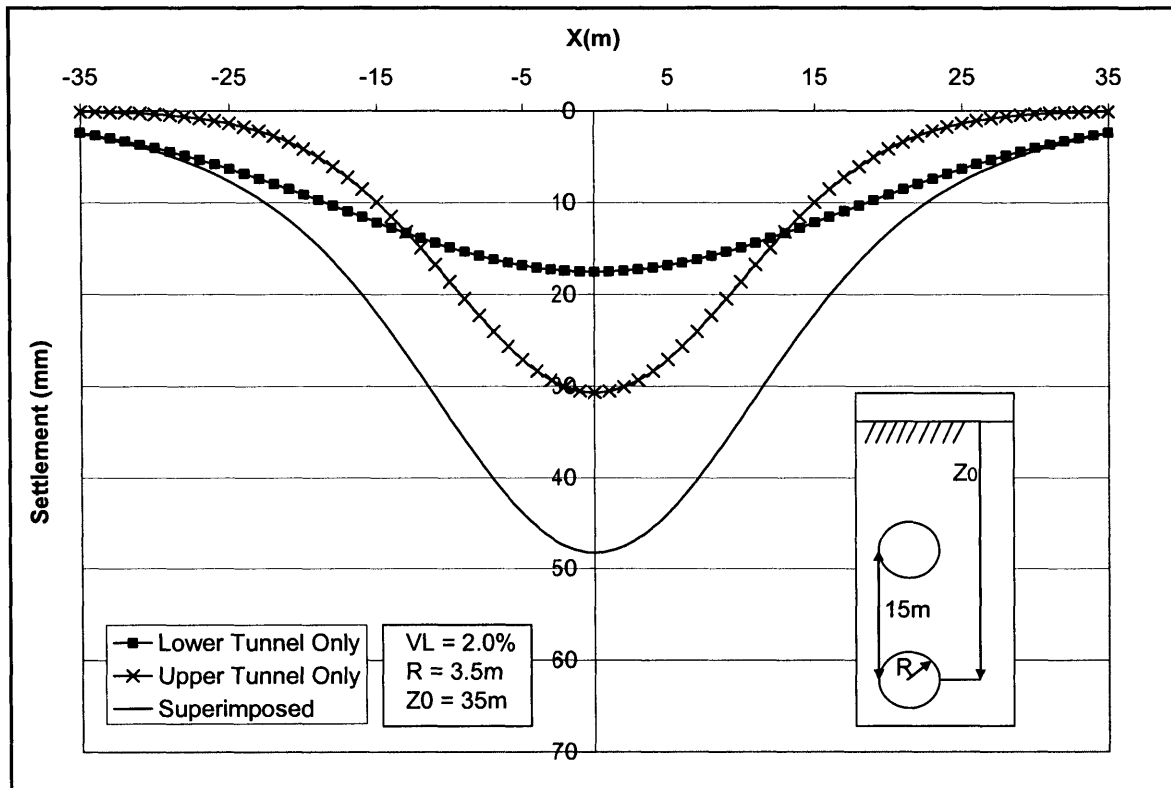


Figure 10. Settlement trough for piggyback tunnels by superposition of empirical equations (Equation 3).

Since the upper tunnel is the one that causes more settlement and therefore the most damage, it is more logical to place the upper tunnel as low as possible. This will create a problem of changing the bending moment in the existing tunnel. Therefore a solution will be looked at in the finite element section (chapter 4) for optimizing the design based on the induced bending moment and the distance between the tunnels.

It is not easy to reduce the settlement in piggyback tunnels because depth is a limiting factor. In side by side tunnels this poses less of a problem as you can move the tunnels farther and farther away from each other without having to go deeper, hence the interaction effects can be significantly reduced with relatively low increase in cost.

Angular-offset Tunnels

If there was inadequate space for a side-by-side or piggyback tunnel, a third option would be to locate the second tunnel at an angular-offset position. The current example assumes the two tunnels are aligned at 45° to each other, and varies the spacing, X_t . As with piggyback tunnels, the issue arises of which tunnel should be constructed first, which will not be addressed in empirical superposition. Figure 11 shows the effects of distance between the tunnels on S_{max} , assessed with the first tunnel located at $Z_0 = 35$ and the second at depths ranging from 24m to 10m.

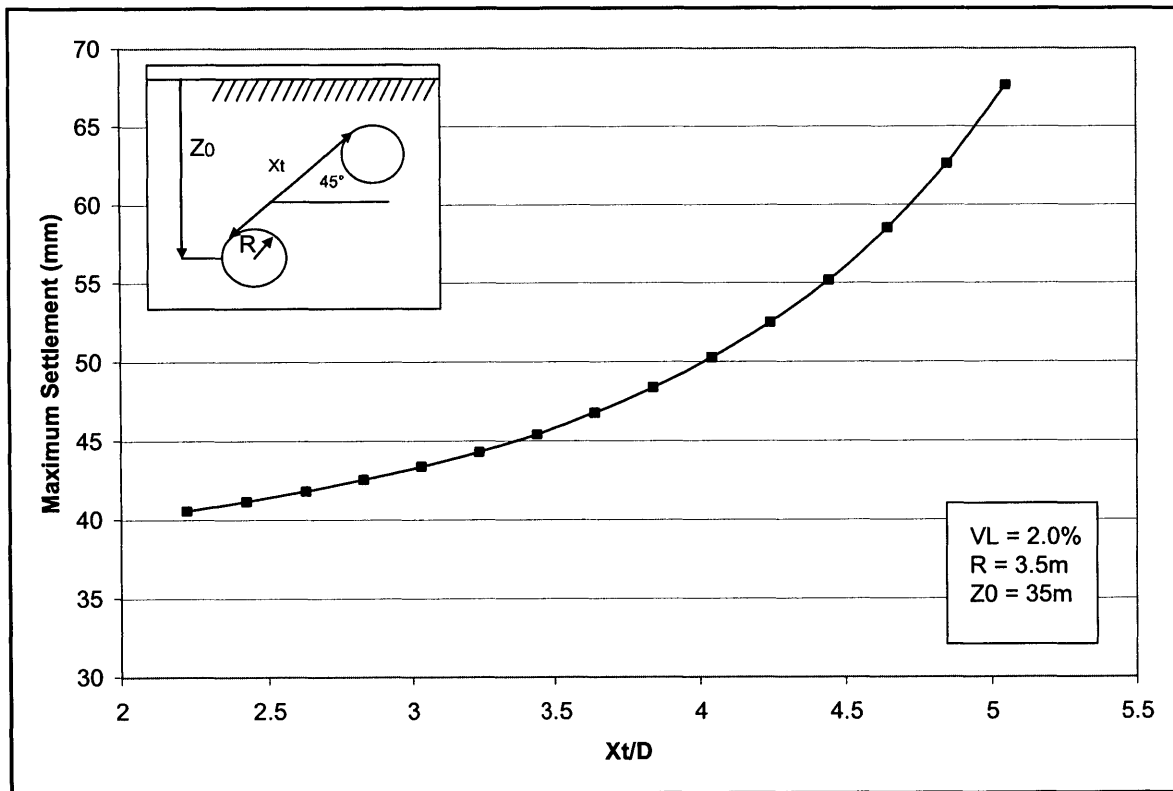


Figure 11. Effect of distance between angular tunnels on S_{max} using superposition of empirical equations (Equation 3)

This creates a similar graph to the piggyback tunnels but with some key differences. The combined settlement is much lower in this method (e.g. for $X_t/2R \approx 2$, $S_{max} = 75\text{mm}$ and 45mm for piggyback and angular-offset configurations, respectively). It is possible to construct the tunnel much farther away ($X_t/2R < 5$) here at an angular-offset of 45° .

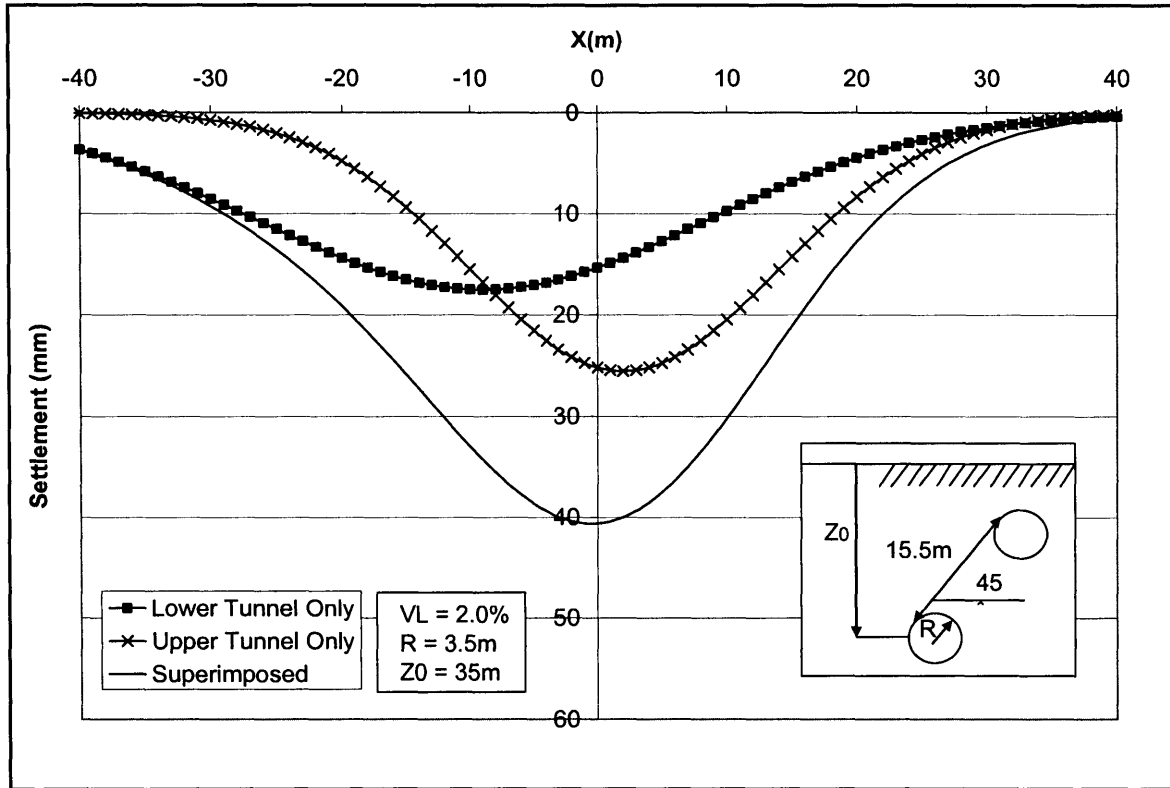


Figure 12. Empirical settlement trough for angular-offset tunnel using superposition of empirical equations (Equation 3).

Figure 12 shows the empirical settlement trough for angular-offset tunnels at 45° with the first tunnel at 35m depth and the second at 24m depth. The settlement above the lower tunnel is much less than the settlement above the upper tunnel, therefore when the superimposed curve is created the maximum settlement is almost directly above the upper tunnel. During design angular tunnels the upper tunnel should be positioned where the resulting settlement would cause the least damage.

3.2.2 SUBSURFACE EFFECTS

The vertical settlement troughs for the subsurface are very similar to the settlement troughs for the surface, therefore there is no need to plot the data again as we can assume that the same patterns will be seen in the subsurface. However, it is still important to consider the lateral movement throughout the soil for the same three situations used in section 3.2.1: 1) a side-by-side tunnel 2) a piggyback tunnel and 3) a 45° angular-offset tunnels. For this section equation 11 (Attewell et al, 1986) is used to superimpose lateral movements in soil.

Side-By-Side Tunnels

In this situation, due to the principal of superposition it is assumed that for values of x directly in the centre of the two tunnels the lateral movements will be zero. Therefore the values will be found only for directly above each tunnel. Figure 13 shows the lateral movement with depth, estimated above each tunnel.

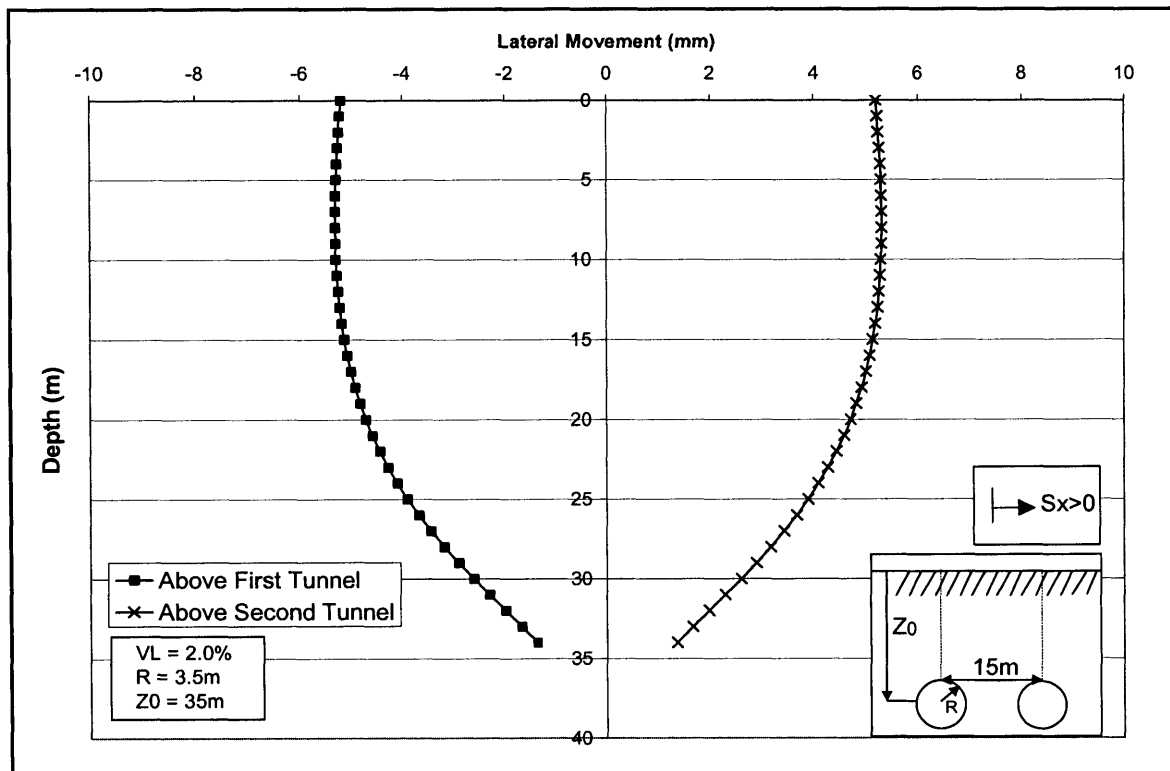


Figure 13. Lateral Movements with depth for side-by-side tunnels using superposition of empirical equations (Equation 11).

From Figure 13 it can be seen that the estimated deflections above each tunnel are equal in magnitude and opposite in direction. At the center of the first tunnel there is no movement caused the construction of the first tunnel, so the movements which will occur are caused solely by the construction of the second tunnel, and similarly the movements above the second are caused solely by the construction of the first tunnel. Figure 14 shows the lateral movement between the tunnels at 35m depth.

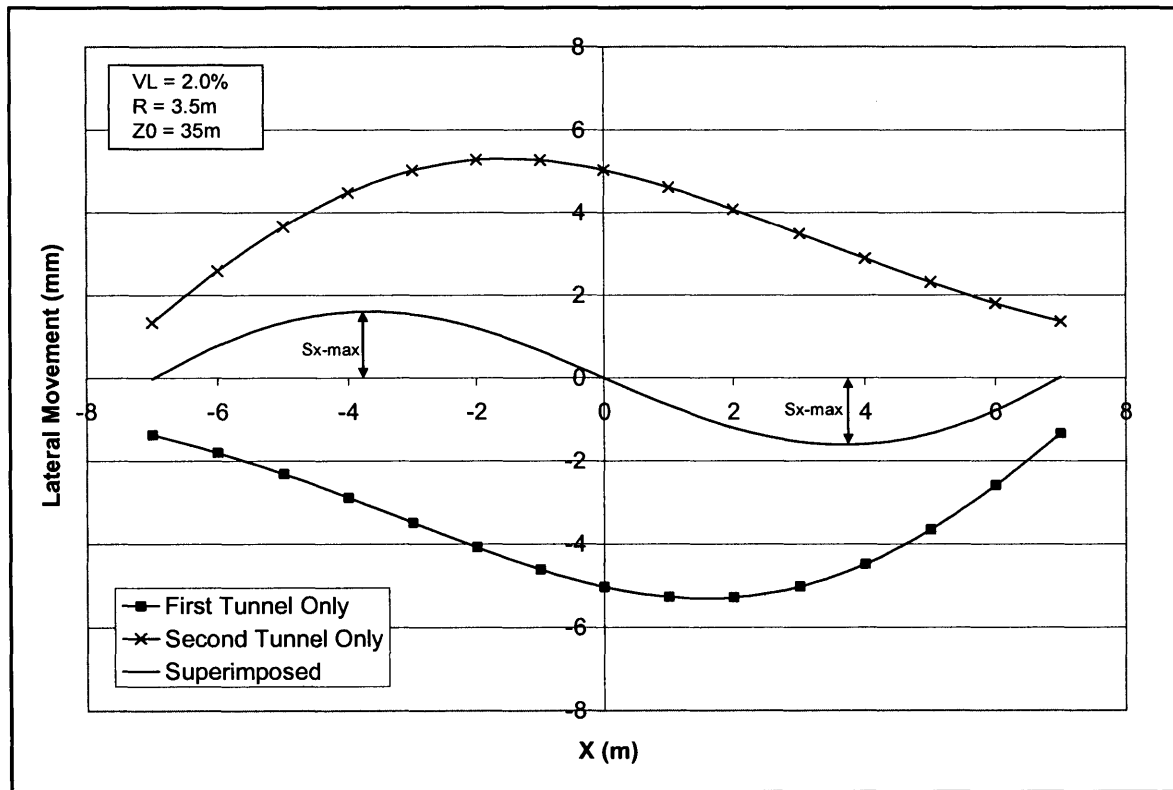


Figure 14. Lateral movements estimated between side-by-side tunnels using superimposition of empirical equations (Equation 11).

Using this method the maximum lateral movements are estimated to occur at one quarter of the distance between the tunnels, in each direction. The final movements that occur as a combination of both tunnels are smaller than the movements which occur for each tunnel separately. Although this appears satisfactory, the soil is in fact moving for one tunnel and then back as the second tunnel is constructed.

Piggyback Tunnels

Since lateral movement above the centerline of each tunnel is zero there will be only vertical deformations between these tunnels. The effect seen in the side-by-side tunnels where the lateral movements 'cancel out' will not be seen here, which means that the net lateral movements will be accumulative. In Figure 15 the lateral deformation is plotted with depth at $x = 10\text{m}$.

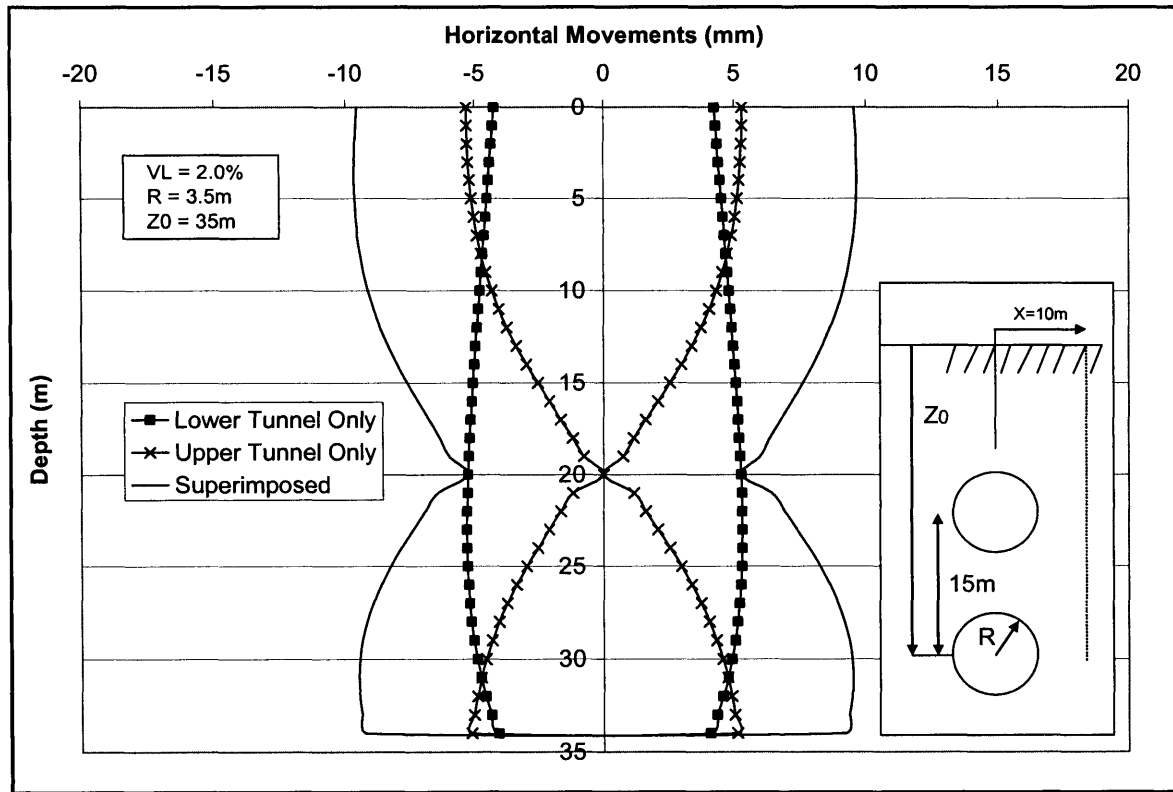


Figure 15. Lateral deformations for piggyback tunnels at $X=10\text{m}$ using superimposition of empirical solutions (Equation 11)

The maximum lateral movement for piggyback tunnels is $\sim 10\text{mm}$ which occurs quite close to the surface in this example. The lateral movement increases with distance until it peaks then begins to decrease.

Angular-Offset Tunnels

For angular-offset tunnels there will be effects from the piggyback and side-by-side tunnels. Figure 16 shows the lateral deformations at the horizontal midpoint between the two tunnels (5.5m from each tunnel).

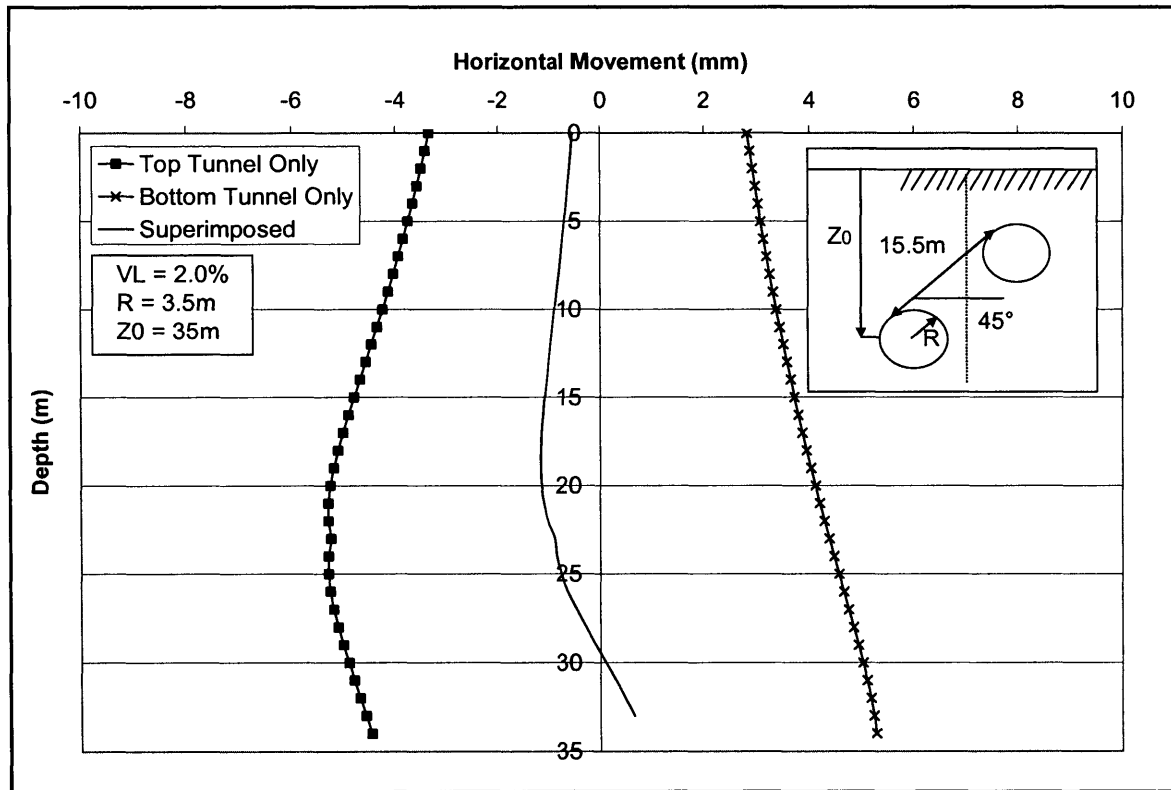


Figure 16. Lateral deformations for angular tunnels.

The superimposed movement is quite similar to that of the side-by-side tunnels, that is, it is close to zero. The lateral movements tend towards the nearest tunnel, so above a depth of 30m they upper tunnel is more influential but at a depth of ~30m the influence switches to the lower tunnel as the ground movements tend towards it.

4.0 FINITE ELEMENT ANALYSIS OF TWIN TUNNELS IN SINGAPORE MARINE CLAY

Plaxis is a finite element program used for soil and rock analyses, it is used in this section to analyze the same situations as outlined in the empirical methods. This section breaks down into the analysis of ground movement and the analysis of the stresses in the tunnel lining.

4.1 GROUND MOVEMENTS

In order to use Plaxis, soil properties and lining properties must be defined. For the soil, Singapore Marine Clay will be used and properties for a typical concrete liner will be taken. Other assumptions used in the analysis are as follows:

- Water table is at ground level
- The volume loss parameter is fixed, $V_L = 2\%$

The soil and lining properties are detailed in Table 2 and Table 3 respectively.

Table 2. Properties of Singapore Marine Clay

General Properties	γ_{sat}	16.8kN/m ³
	K_0	0.7
Stiffness	E	1.3e4kN/m ³
	ν	0.25
Strength	c'	5kN/m ²
	ϕ'	0°
	Y_{ref}	0m
	$C_{\text{increment}}$	1.47kN/m ² /m

Table 3. Properties of Lining

EA	1.47e7kN/m
EI	1.43e5kNm ² /m
d	0.35m
w	8.4kN/m/m
ν	0.15

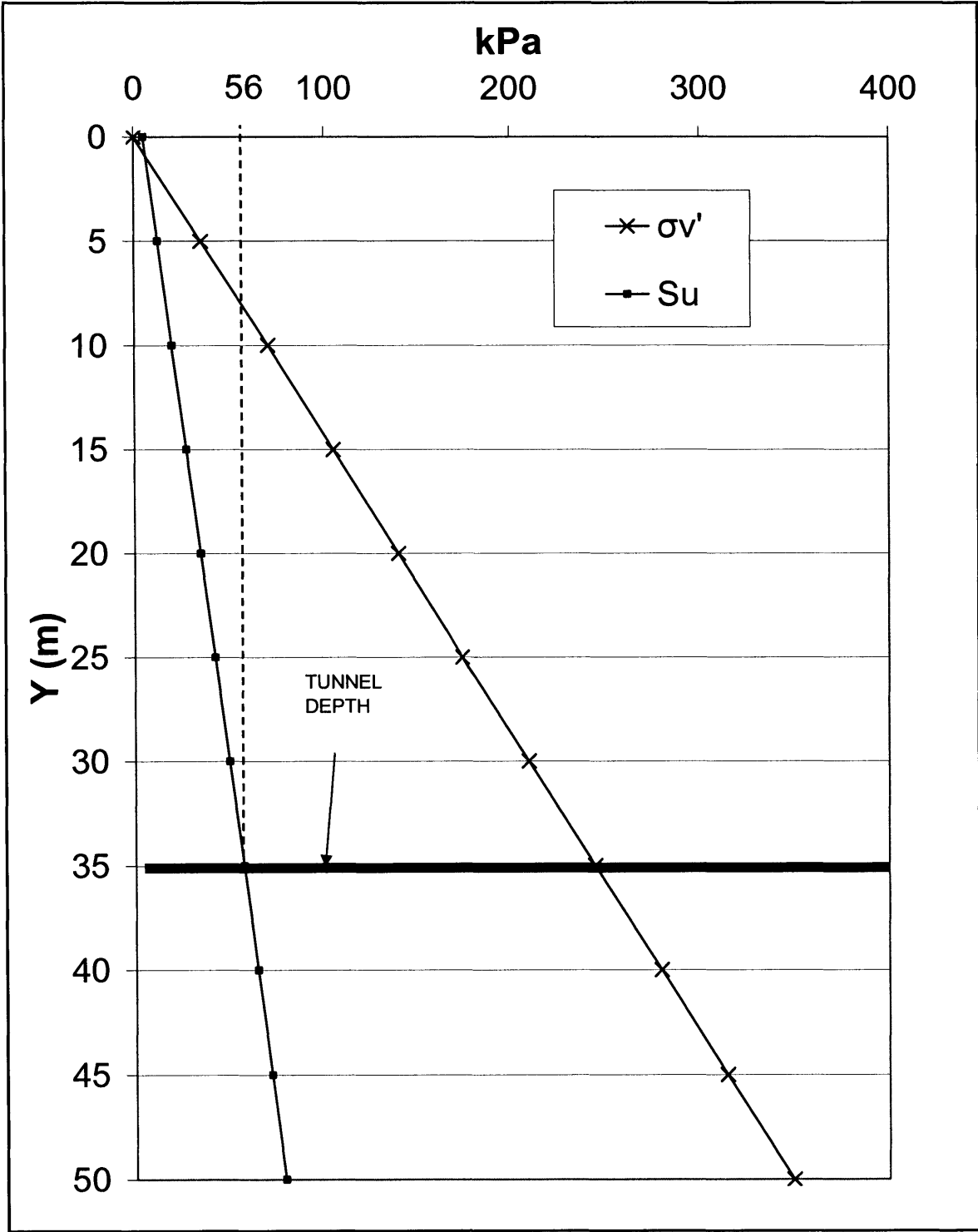


Figure 17. Soil Properties with depth

4.1.1. SURFACE EFFECTS

In order to check that superposition is applicable in tunnel design the settlement troughs for each tunnel are found separately and then superimposed. An analysis will then be run for both tunnels and the resulting trough will be compared to the superimposed trough.

Side-By-Side Tunnels

Figure 18 shows the effect of distance on the maximum settlement. The nearer the tunnels are the larger the settlement is, but at a certain distance the maximum settlement will not decrease further, which corresponds to S_{max} for a single tunnel.

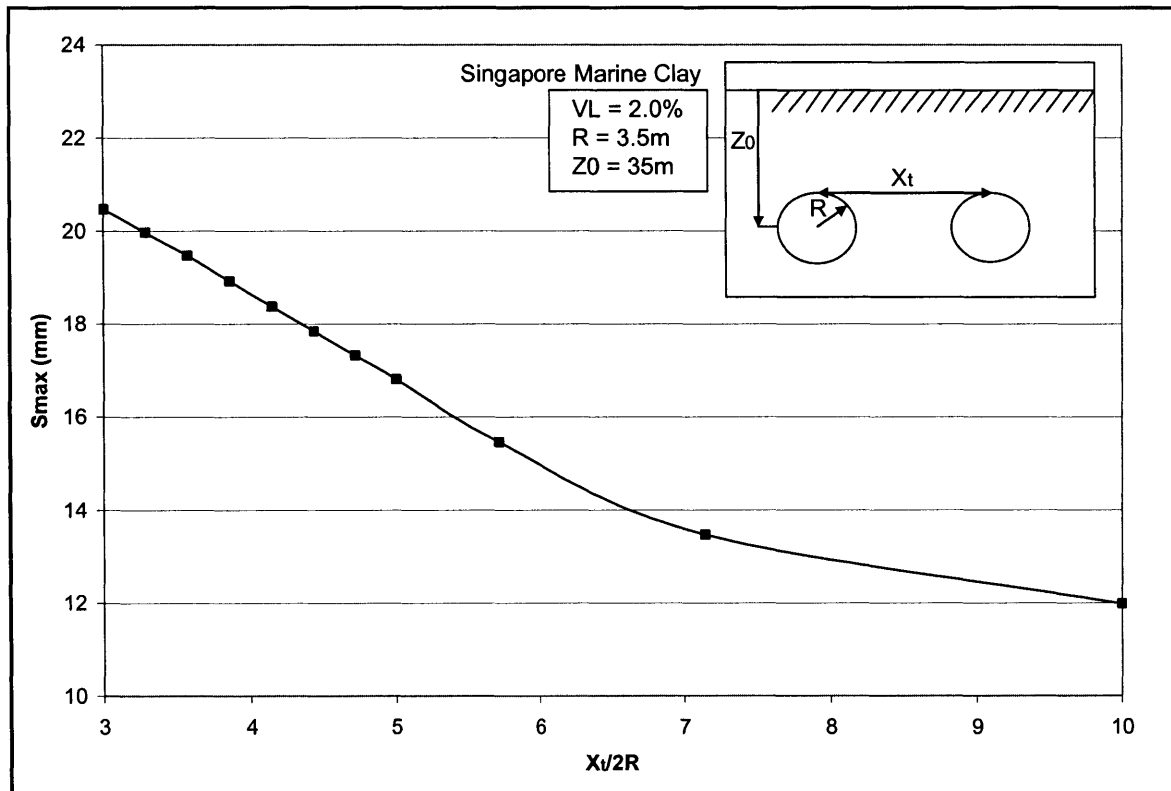


Figure 18. Effect of distance between tunnels on S_{max} .

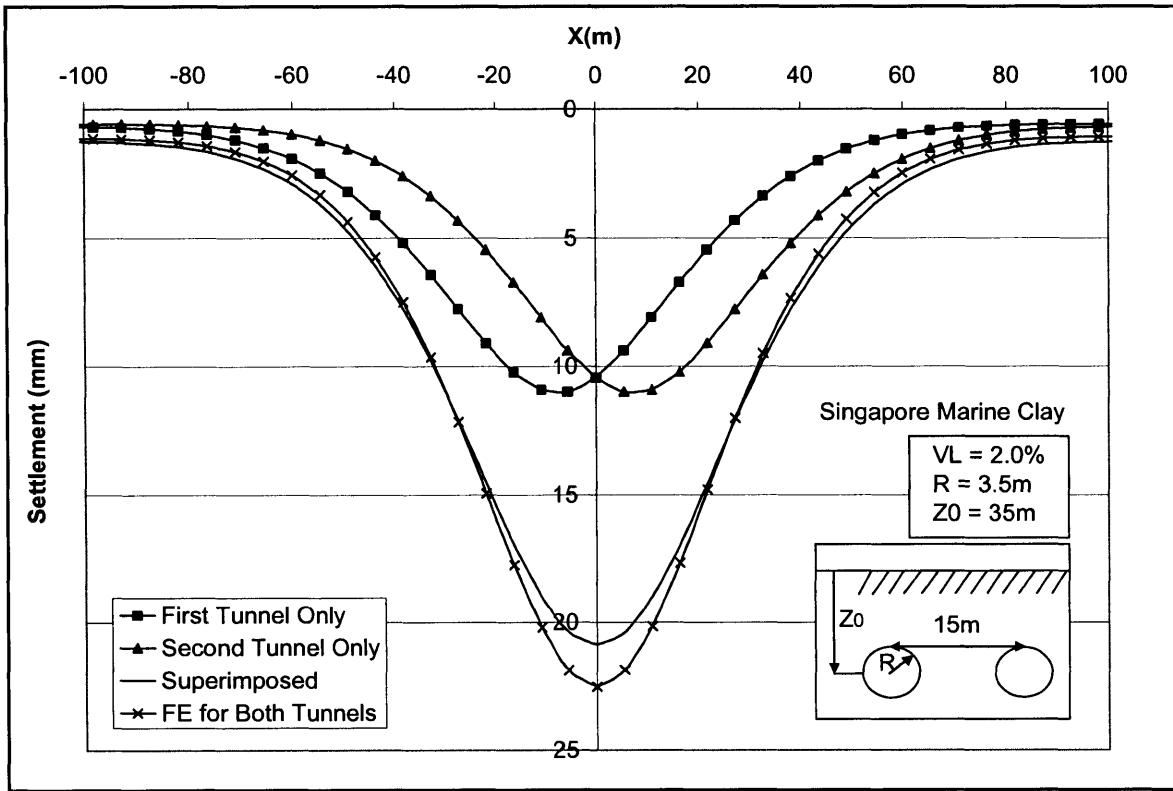


Figure 19. FE Settlement troughs for side by side tunnels ($X_t=15m$)

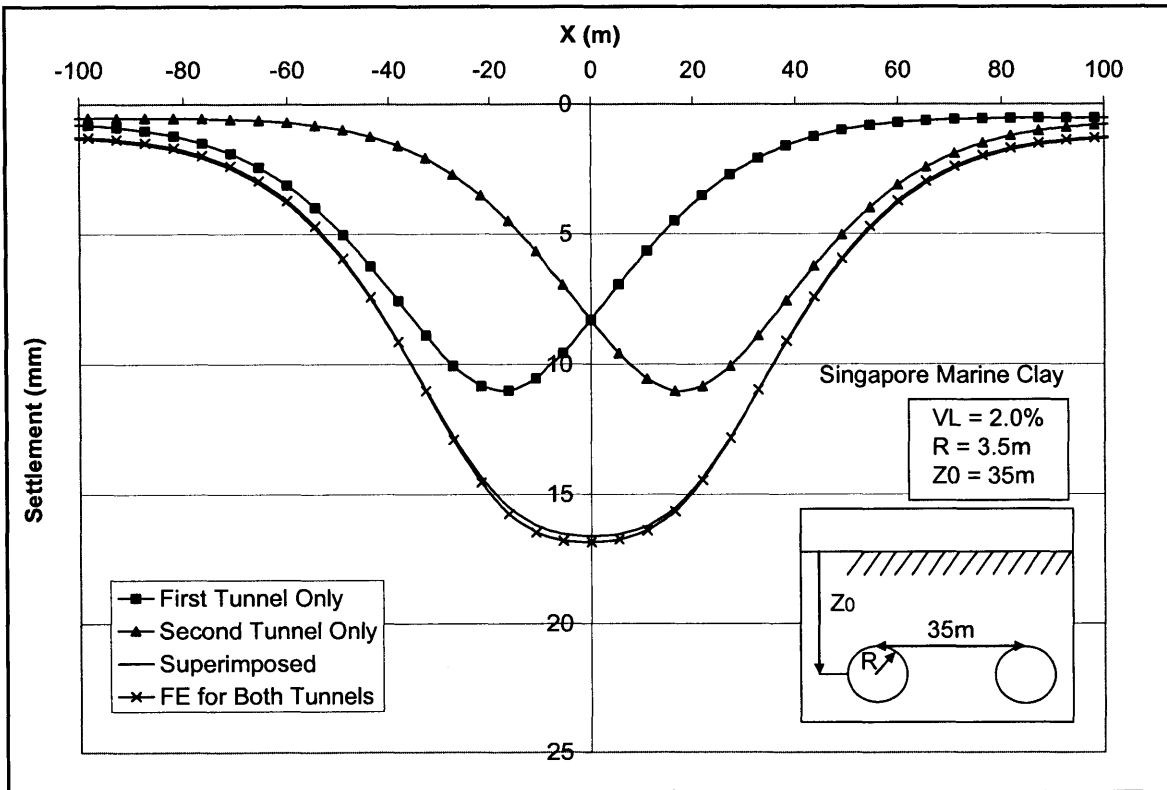


Figure 20. FE settlement troughs for side-by-side tunnels ($X_t = 35m$)

Figure 19 and 20 show side-by-side tunnels for tunnels spaced at 15m and 35m, respectively. For the closely spaced tunnels ($X_t = 15m$) the superimposed curve almost exactly matches the numerical results. Superimposition over-estimates S_{max} by 2mm. Even if there is a small difference superposition obviously works well for closely spaced tunnels. Figure 20 shows a similar chart for widely spaced tunnels ($X_t = 35m$), the superimposed and FE curves align a lot closer in this chart, although there is a fraction of a millimeter difference at the trough, so superposition works very well for closely and widely-spaced side-by-side tunnels.

Piggyback Tunnels

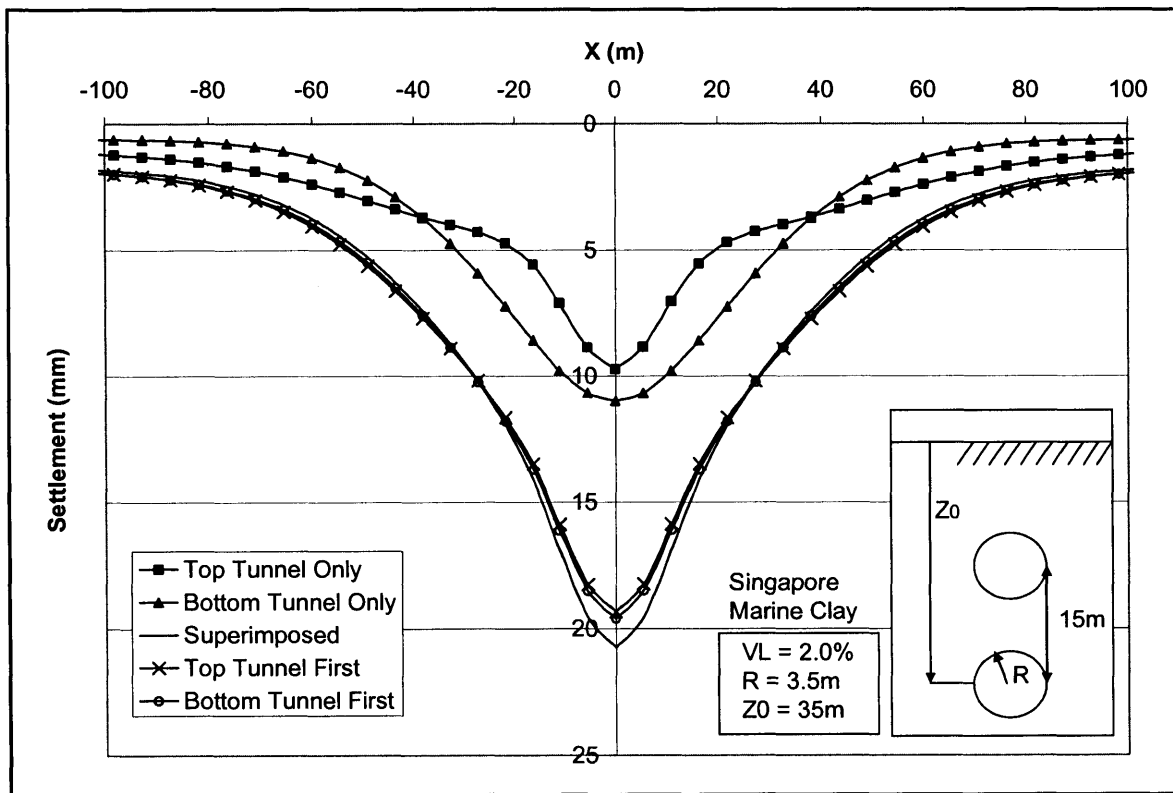


Figure 21. FE Settlement troughs for piggy back tunnels ($X_t = 15m$)

For the finite element analysis of piggyback tunnels two situations have to be considered, one for the top tunnel constructed before the bottom tunnel and one for the bottom tunnel constructed before the top. In Figure 21 both of these situations have been plotted with the superimposed trough.

The trough for constructing the upper tunnel first and the trough for constructing the lower tunnel first are very close together and gave a result for the maximum settlement of 19mm. Therefore, the order of construction has very little effect on the final settlement trough, in this example. The results show less than 2mm difference in the maximum settlements compared to direct superposition settlement and practically identical results for $X > 25\text{m}$.

In a separate set of analyses the maximum settlement was checked for varying values of X_i , the distance between the piggyback tunnels. The results show very little variation in the maximum settlement as the upper tunnel was progressively moved from a depth of 20m to a depth of 10m. The settlement occurring was ~19mm with a variance of ~1mm. This shows that, in finite element analysis, the vertical effects of piggyback tunnels do not interfere significantly with the maximum settlement.

Angular-Offset Tunnels

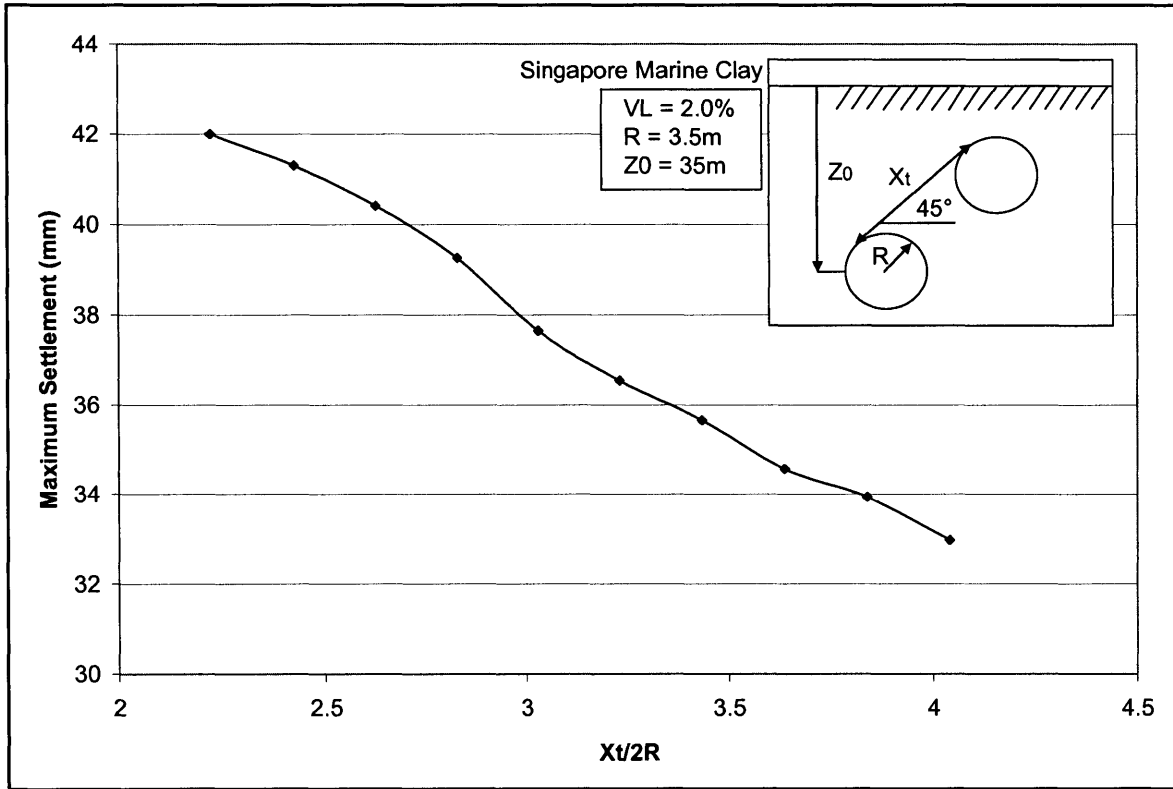


Figure 22. Effect of distance between angular tunnels on S_{max}

Figure 22 shows the maximum settlement computed for varying distances between two 45° angular-offset tunnels. The results show a linear decay with spacing between the two tunnel bores.

However, looking at the trends for side-by-side and piggyback curves, the maximum settlement would be expected to reach its minimum value at $X_t/2R \approx 10$, so for a 45° angle in order to achieve this the lower tunnel would have to be at a depth, $Z_0 > 50m$.

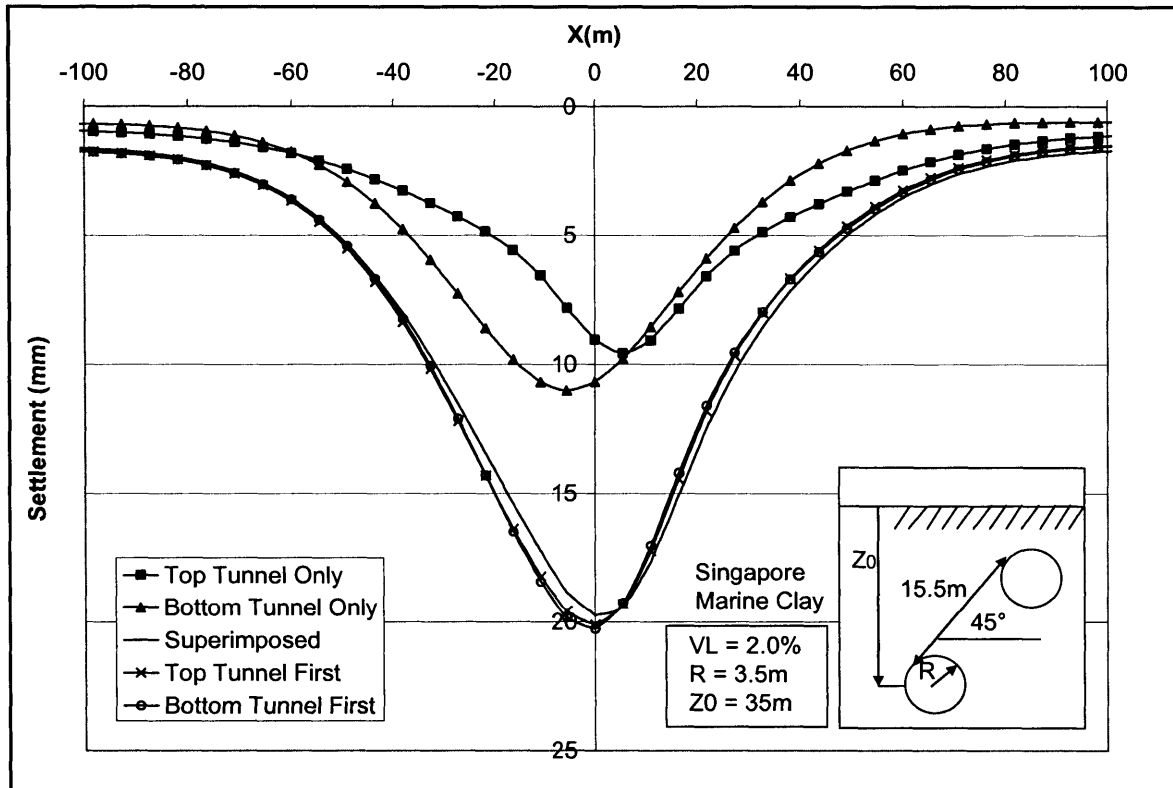


Figure 23. FE settlement troughs for Angular Tunnels ($X_t=15\text{m}$)

Similarly to the piggyback tunnels there is an issue with the order of construction of angular-offset tunnels. Fig 23 shows the troughs for each situation.

The surface settlement troughs for constructing tunnels in different sequences are very similar and produce settlement differences less than 2mm. This shows that the order of construction has no effect on the final settlement trough for the soft clay conditions considered in this case.

The superposition curve is almost identical to the trough for constructing the lower tunnel first and very close to the trough for constructing the upper tunnel first. Therefore, it can be seen that superposition works extremely well when estimating settlement for the 45° angular-offset tunnels.

4.1.2 SUBSURFACE EFFECTS

Considering that the vertical settlement profiles with depth are very similar to the settlement profiles for the surface it can be assumed that similar patterns will be seen. This section compares the lateral movements estimated by Plaxis, and determines whether or not the principle of superposition can be applied based in non-linear finite element analysis.

Side-By-Side Tunnels

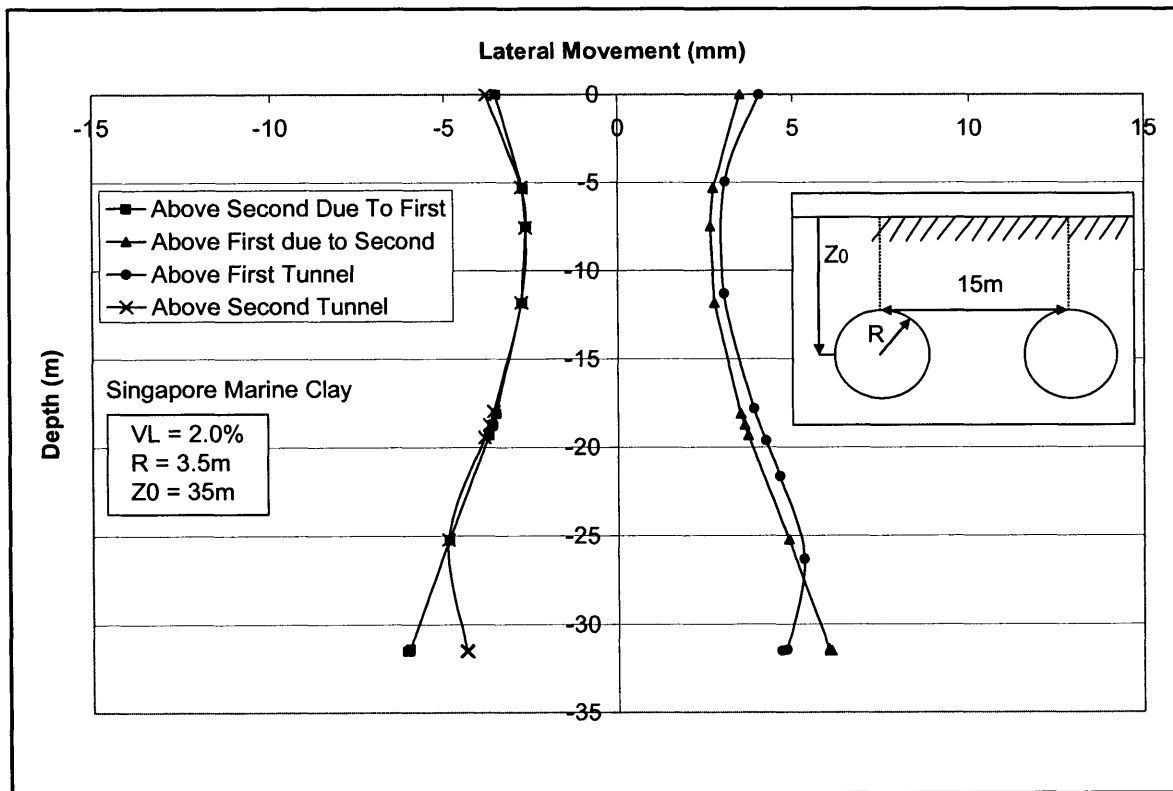


Figure 24. FE Lateral movements with depth for side-by-side tunnels

In Figure 24, it can be seen that the lateral movements above the first tunnel are almost symmetrical to the lateral movements above the second tunnel, with the largest variance being ~1mm. Considering that there are zero lateral movements above each tunnel due to the construction of that tunnel and that the effects of the opposite tunnel are very close to the final settlement, this shows that superposition works.

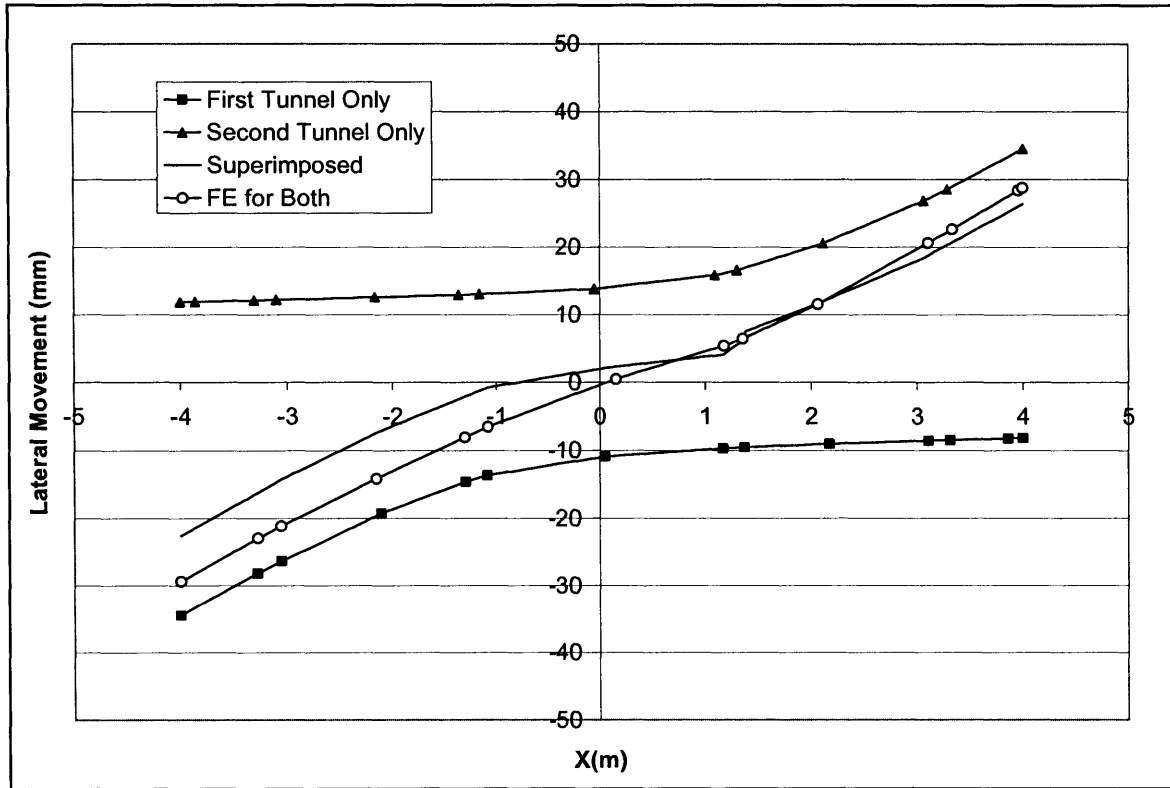


Figure 25. FE Lateral movements estimated between side-by-side tunnels

In Figure 25 the lateral movements were calculated for the space between the tunnels. It can be seen that when combined, the lateral movement calculated exactly in between the tunnels is zero. The superimposed curve roughly aligns with the finite element curve for the second tunnel, however, near the first tunnel there is a significant discrepancy ($S_x = 7\text{mm}$). In this zone between the two tunnels, the plastic zones for each tunnel will intersect, which will almost always cause severe plastic deformation. Therefore, superposition will suggest approximate results but is not very accurate, in this example.

Piggyback Tunnels

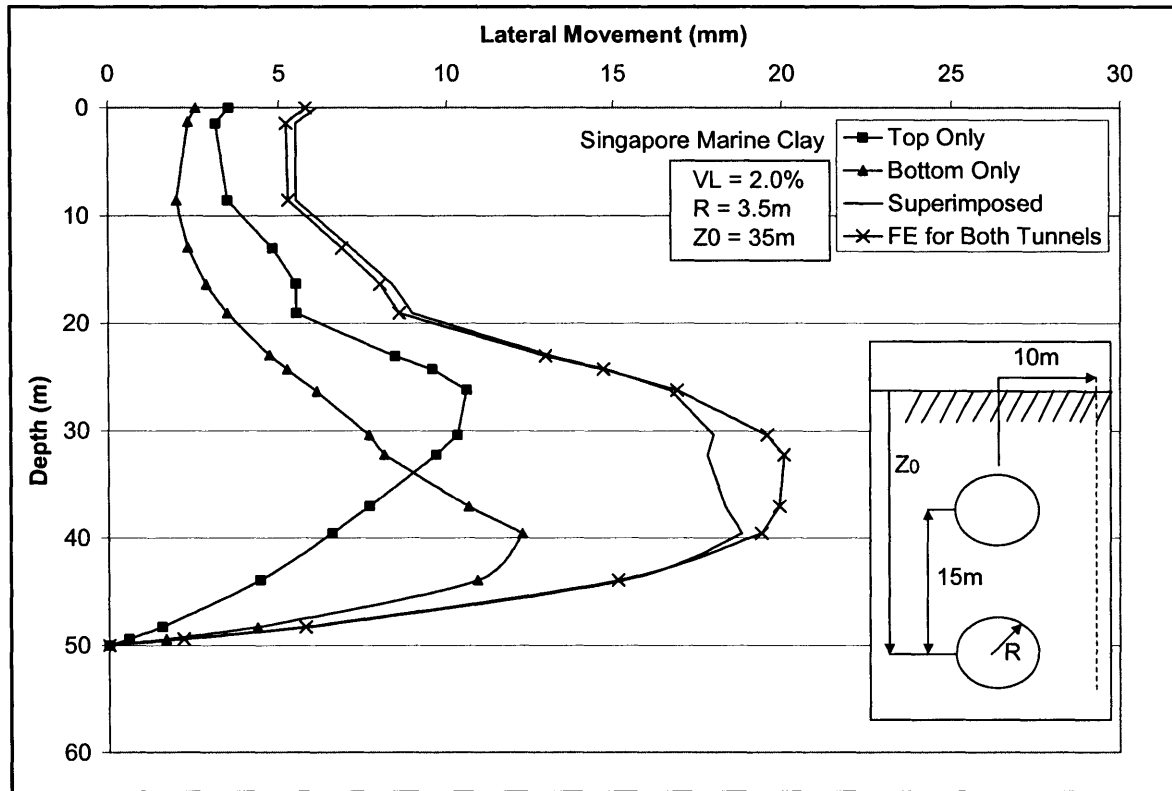


Figure 26. FE Lateral deformations for piggyback tunnels ($x = 10\text{m}$)

For piggyback tunnels, the lateral deformations were estimated for a vertical profile at a horizontal distance of 10m. These movements will be symmetrical on the other side of the tunnel centerline. For the upper tunnel only, the minimum movement occurs at the level of the tunnel (at depth of 20m) whereas for the lower tunnel only the minimum movement occurs much nearer the surface. Regardless of this, the superimposed curve matches the combined curve within ~1mm until a depth of about 30m where the combined FE analysis begins to gradually increase with respect to the corresponding superimposed value.

Angular-Offset Tunnels

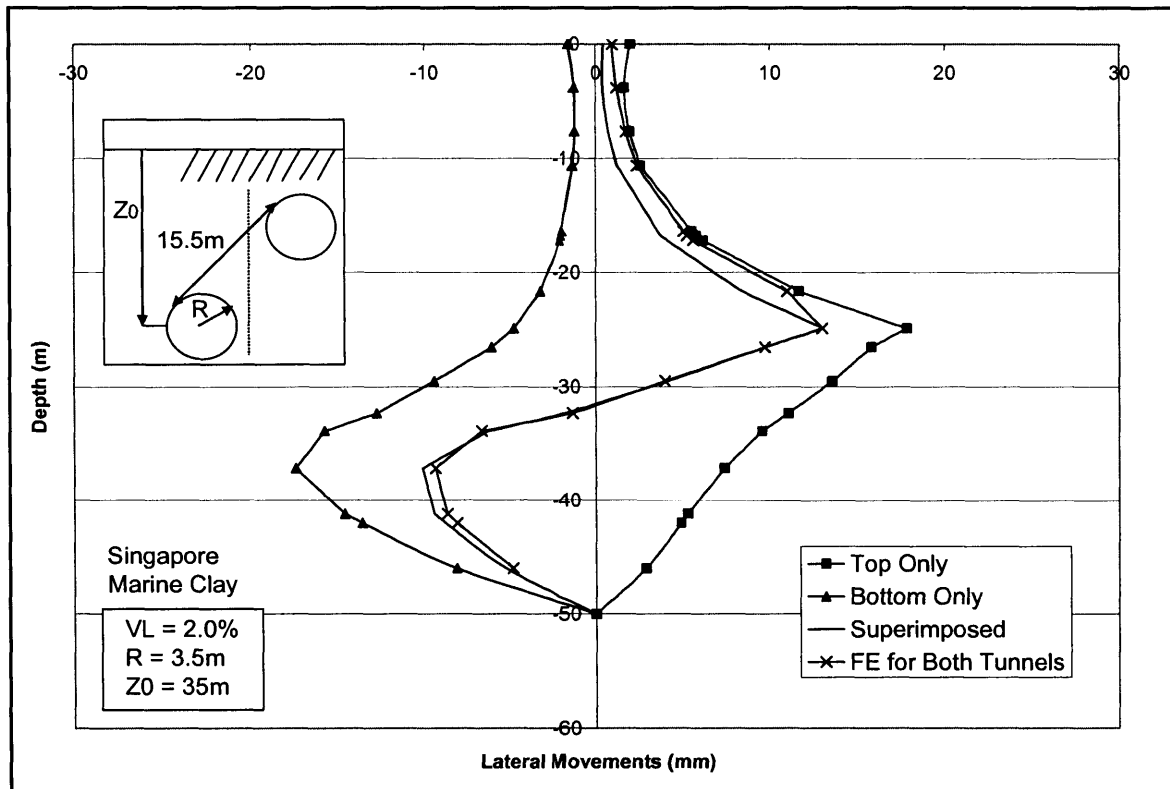


Figure 27. FE Lateral deformations for angular tunnels

In order to compare the lateral movements for angular tunnel, the estimates were made for the lateral mid-point between the two tunnels. The profiles for each tunnel individually are of a very similar shape, though the lower tunnel does induce slightly more movement than the upper (~1mm). The superimposed curve compares very well to the finite element curve, especially in the zone of depth between the two tunnel elevations. However, superposition is clearly less accurate for depths less than 24m but remains a good first approximation for angular-offset tunnels.

Plastic Deformations

The comparison between the superimposed solutions and the finite element solutions illustrate that superposition applies very well to these situations. The discrepancies that occur in the solution are caused by the plastic deformation that occurs in the soil immediately surrounding the tunnels. In Figure 28, the plastic zone for twin tunnels located at 15m from centerline to centerline is shown.

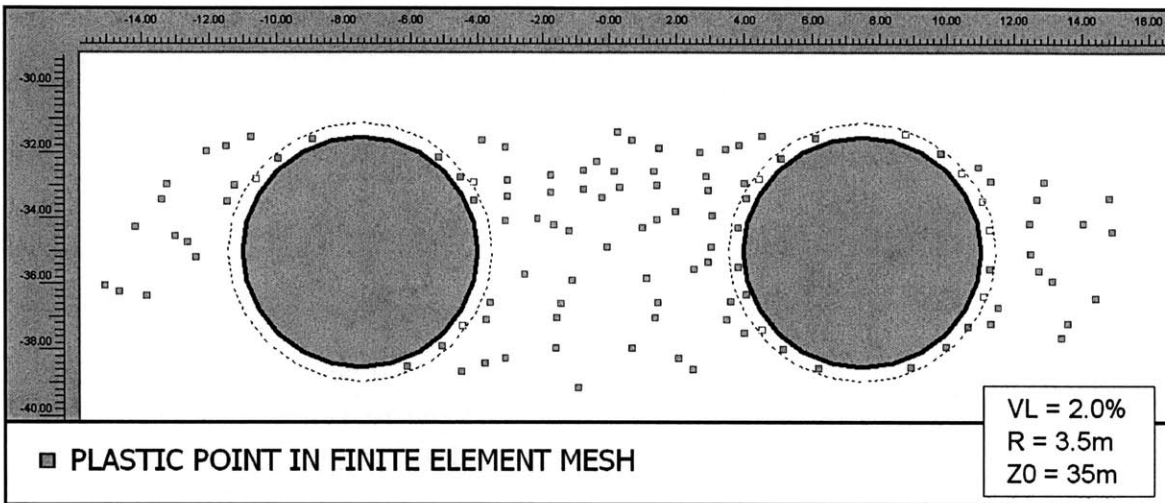


Figure 28. Plastic Zone surrounding side-by-side tunnels ($Xt/2R = 2.2$).

The zone of plasticity surrounding each tunnel is roughly equal to the radius of the tunnel (3.5m). Using this zone of plasticity and comparing it to Figure 18, it is seen that the location of the largest difference between the curves corresponds to the centre of the combined plastic zone from the two tunnels. Similarly for the piggyback and angular situations the plastic zones correspond to the areas where superposition breaks down.

4.2 LINING STRESSES

Estimates of surface settlements due to tunneling are very important in order to mitigate potential damage to adjacent structures. However, it is also very important to predict the expected forces and deformations that will be seen in the adjacent tunnel lining so that the correct design can be made for the tunnel. For example, in an underground subway tunnel, if the tunnel deforms more than expected or if the bending moment induces a crack in the lining then the functionality of the tunnel is compromised. This section consists of structural lining interaction between twin tunnels. The same examples that were used in the previous sections are used again.

The force used to measure and compare each situation is the bending moment in the liner, which is plotted against varying values of $X_i/2R$. For each analysis there are three bending moments which are:

- Bending moment in the first tunnel due to the construction of the first tunnel
- Bending moment in the first tunnel after the construction of the second tunnel
- Bending moment in the second tunnel due to the construction of the second tunnel

4.2.1 SIDE-BY-SIDE TUNNELS

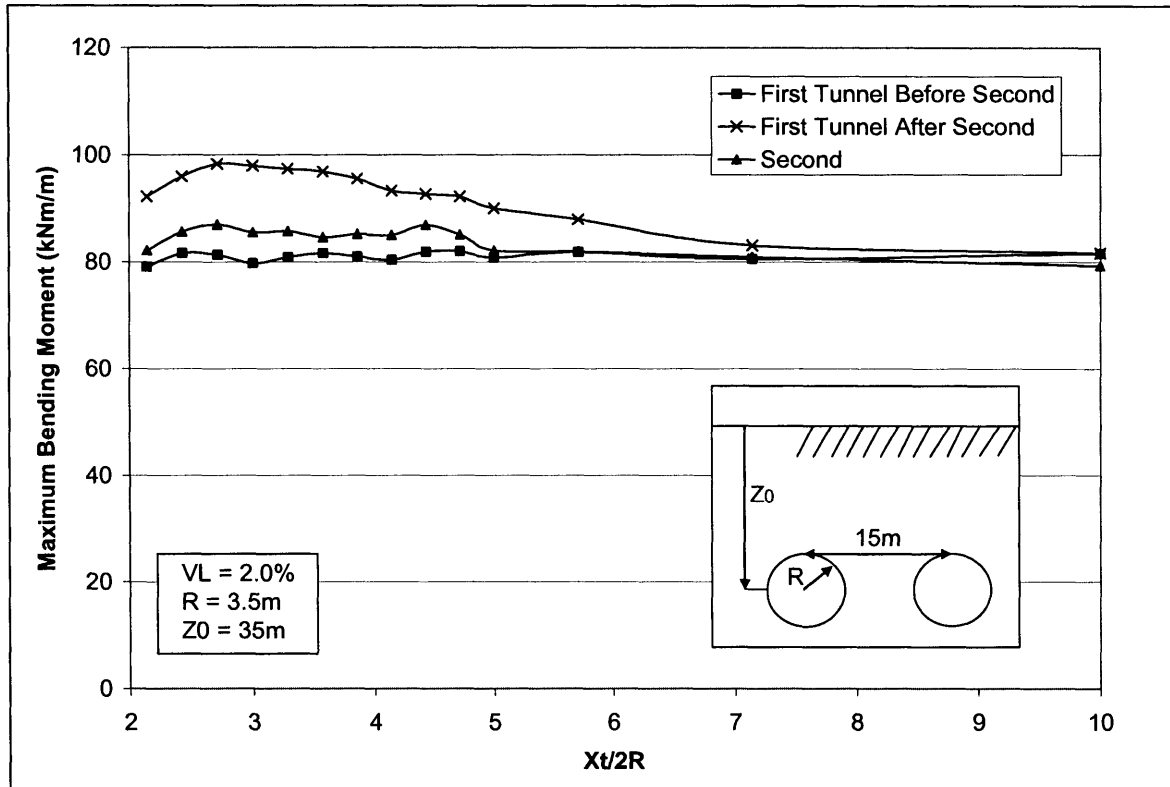


Figure 29. Effect of distance on Bending moments in tunnels

As distance was varied for values of $X_t/2R$ from 2 to 10, the bending moments varied, as seen in Figure 29. For the first tunnel, the bending moment increased from ~ 80 kNm/m to 98 kNm/m at the most critical point. However, the farther the tunnels are placed from each other the less effect they have. For $X_t/2R > 6$, the bending moment in the first tunnel doesn't change due to the construction of the second tunnel. The tunnels are located at the same depth, so if they were built independently, the exact same bending moment should be measured in each lining. In the zone closer to the first tunnel the second tunnel has a slightly higher bending moment.

Moments in Tunnel Lining

The following three figures show the bending moments at each stage of the construction process of a 15m spaced side-by-side tunnel. Figure 30 shows the bending moment in the first tunnel by itself. The maximum moment is seen in the tunnel springline. The moment distribution is symmetrical for this case.

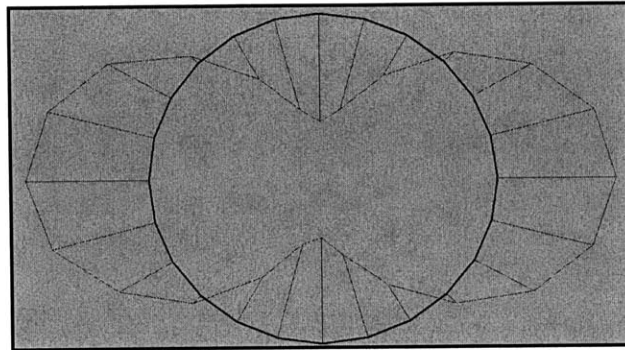


Figure 30. Bending Moment in First Tunnel Only - Max BM = 79.48kNm/m

After the construction of the second tunnel the bending moment diagram changes shape slightly (Figure 31). The maximum moment is now seen in the left springline, on the far side from the new tunnel.

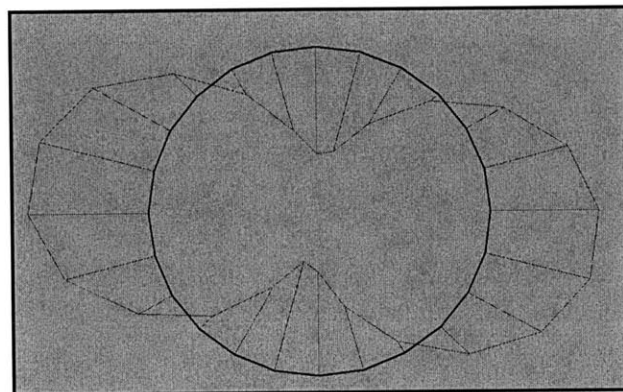


Figure 31. Bending Moment in First Tunnel After second tunnel – Max BM = 93.15kNm/m

Finally, the moment seen in the second tunnel after its construction is shown in Figure 32. The maximum bending moment for the second tunnel is seen in the right springline, located on the far side from the first tunnel.

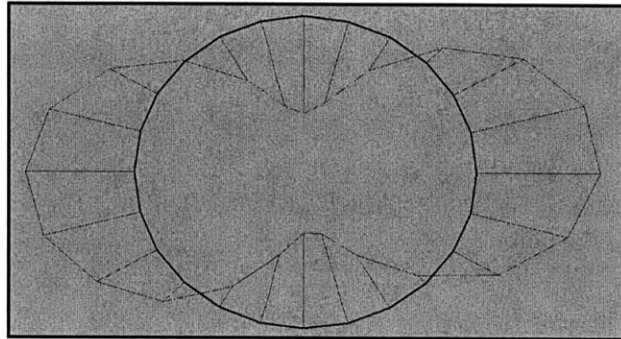


Figure 32. Bending moment in Second Tunnel – Max BM = 82.59kNm/m

4.2.2 PIGGYBACK TUNNELS

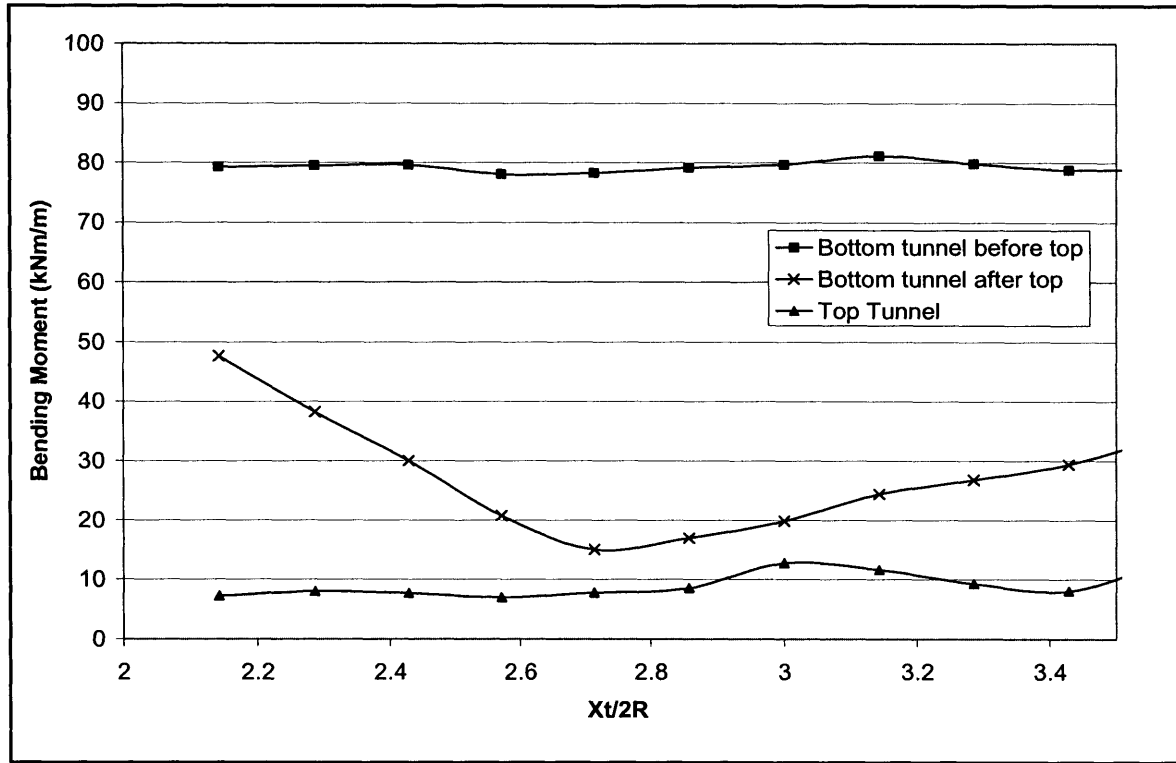


Figure 33. Effect of distance on Bending moments in piggyback tunnels (Bottom First)

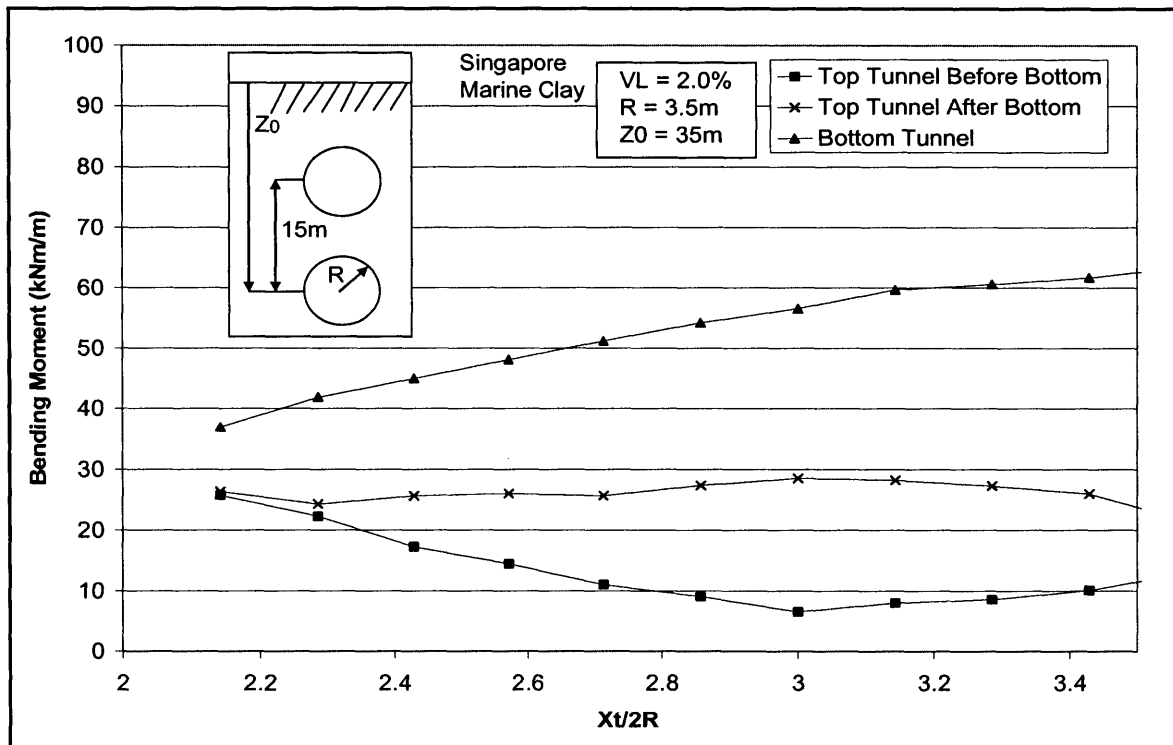


Figure 34. Effect of distance on Bending moments in piggyback tunnels (Top First)

The analysis for the piggyback tunnels is shown in Figures 33 and 34. Figure 29 shows the situation where the bottom tunnel (at $Z_0 = 35\text{m}$) was constructed before the upper tunnel. The location of the upper tunnels varies for $X_t/2R = 2$ to 3.4 such that the shallowest upper tunnel is at $Z = 10\text{m}$. The limit of 3.4 arises from the minimum depth of the upper tunnel of $\sim 10\text{m}$. Figure 30 shows the situation where the upper tunnel was constructed before the lower tunnel, but the location of the upper tunnel was varied exactly as for the situation when constructing the bottom tunnel first.

In Figure 33, the bending moment for the lower tunnel is constant ($Z_0 = 35\text{m}$), but when the upper tunnel is constructed there is a large reduction in the lower bending moment from $\sim 80\text{kNm/m}$ to 15kNm/m , in the most severe situation (an 80% decrease). This trough occurs at $X_t/2R = 2.7$ and at higher values the bending moment is starting to increase. However, since the tunnels cannot be placed at much further distances, the effects cannot be determined.

In Figure 34, the independent bending moment for the upper tunnel increases with depth, and increases significantly after the construction of the lower tunnel. This result occurs due to settlement produced by the construction of the lower tunnel. When the lower tunnel is constructed the upper tunnel will settle further than the ground above it, which will increase the vertical stress and therefore the bending moment in the tunnel lining.

Even though the final stresses are different for both situations, the sum of the maximum bending moments is more consistent. For any value of X_t in Figure 33, if the final moment in the lower tunnel is less than in Figure 34, the moment for the upper tunnel is greater. Therefore, in order to reduce a higher moment in either of the two tunnels, the upper one should always be constructed first.

4.2.3 ANGULAR-OFFSET TUNNELS

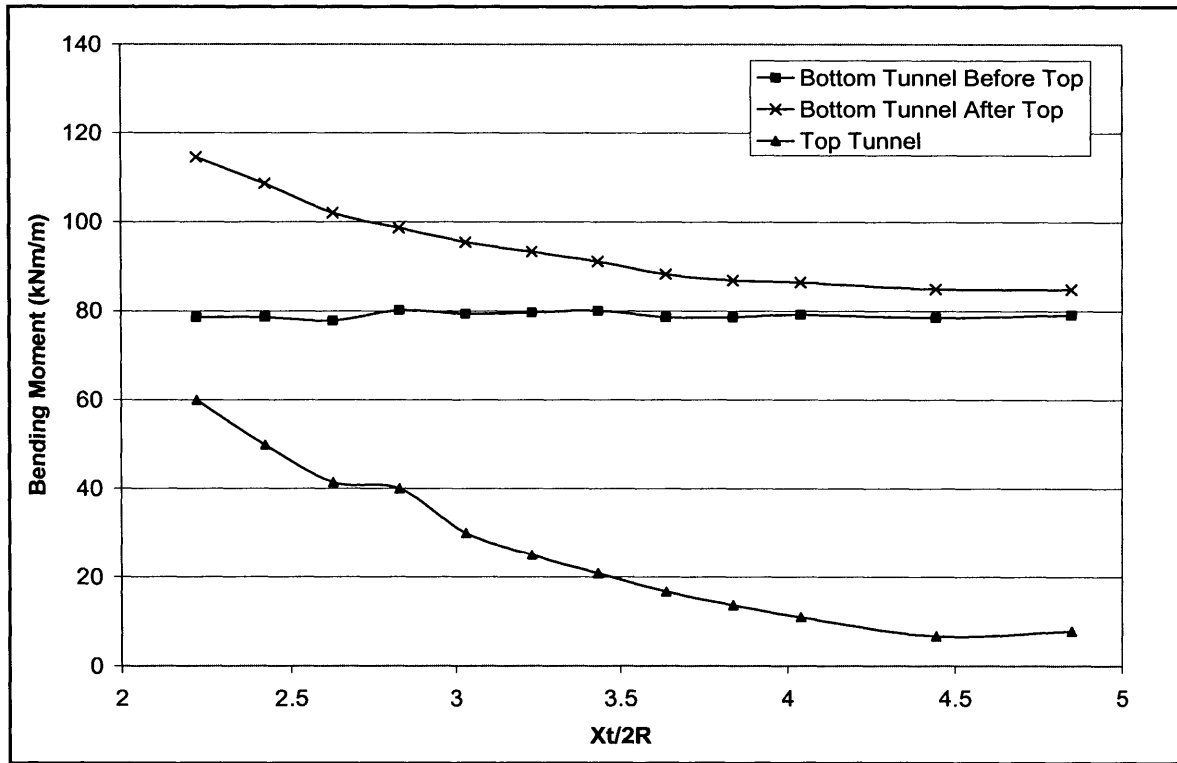


Figure 35. Effect of distance on lining stresses in angular tunnels (bottom first)

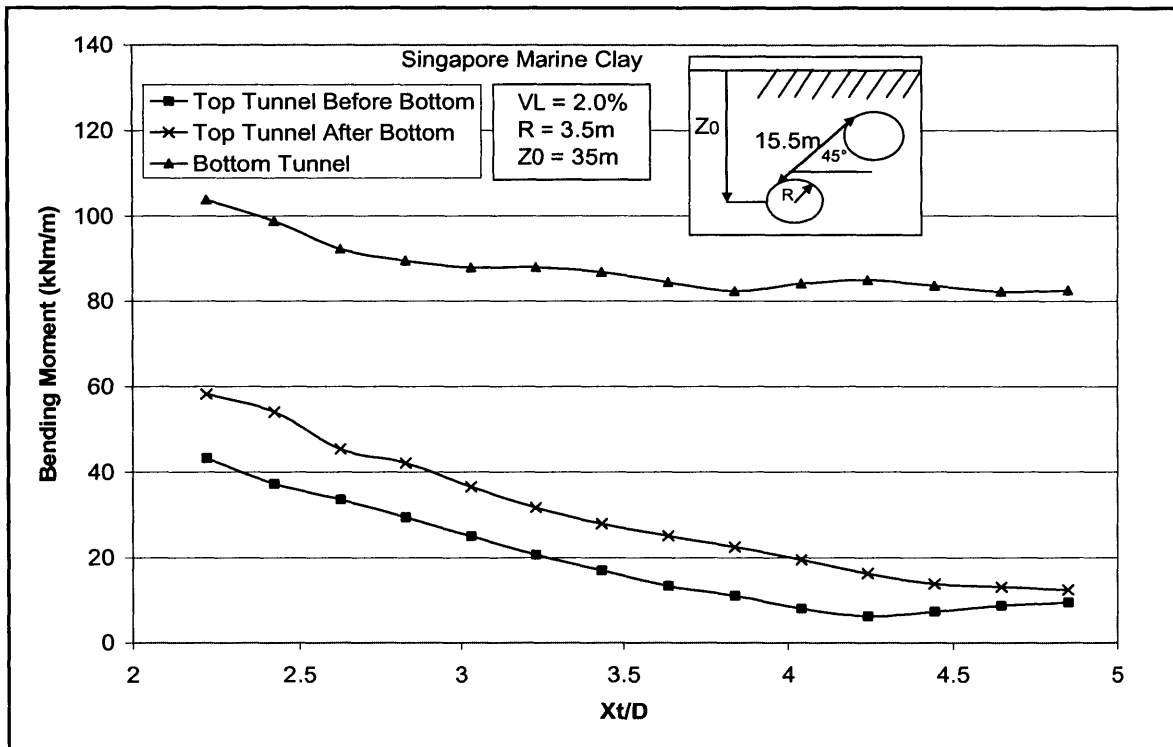


Figure 36. Effect of distance on lining stresses in angular tunnels (top first)

The analysis for the 45° angular-offset tunnels is shown in Figures 35 and 36. Figure 35 shows the situation where the lower tunnel (35m depth) was constructed before the upper tunnel, located at 45° from the horizontal plane. The location of the upper tunnel is varied in the range $X_i/2R = 2$ to 5 (with minimum $Z = 10\text{m}$ for the upper tunnel). Figure 35 shows the situation where the lower tunnel is constructed first.

In Figure 35, the bending moments calculated for the lower tunnel ($Z_0 = 35\text{m}$) $M = 80\text{kNm/m}$. Although unlike the piggyback tunnel, when the upper tunnel is built, the moment in the lower tunnel increases. The largest increase is at $X_i/2R = 2$, where it increases to 116kNm/m (45% increase). As the tunnels are placed at further and further distances apart the increase is reduced to about 5kNm/m (6%).

In Figure 36, the bending moment calculated for the upper tunnel ($Z_0 = 10\text{m} - 25\text{m}$), before the lower tunnel is constructed, varies depending on the depth at which the tunnel is constructed. After the construction of the lower tunnel, the bending moment in the upper tunnel increases by $\sim 18\text{kNm/m}$ until $X_i/2R = 4.2$, when it begins to level out and have no effect. The moment in the lower tunnel ranges from 116kNm/m to a minimum level of 80kNm/m .

Unlike the piggyback tunnels, the final moments calculated in the upper and lower tunnels are very similar. This shows that the order of construction has no significant effect on the bending moments in either tunnel.

5.0 COMPARISON OF NUMERICAL AND EMPIRICAL RESULTS FOR TWIN TUNNELS

This section is directly compares the numerical solutions using non-linear finite element analysis methods (Chapter 4) with empirical methods (Chapter 3).

5.1 COMPARISON OF NUMERICAL AND EMPIRICAL GROUND MOVEMENTS

5.1.1 Side-By-Side Tunnels

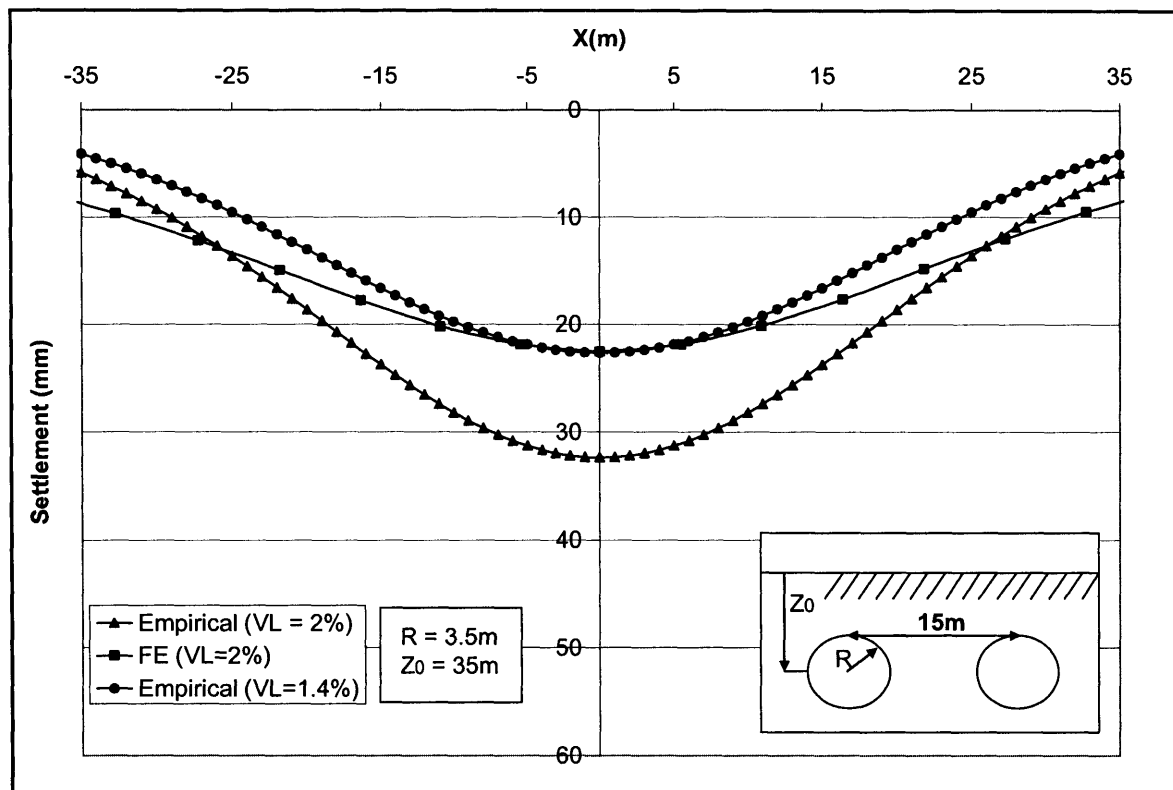


Figure 37. FE vs. Empirical surface settlement trough for side-by-side tunnels

Figure 36 shows the surface settlement for side-by-side tunnels. Directly compared the empirical trough gives a much larger settlement. However, using a V_L of 1.4% which matched the S_{max} for the finite element analysis, a better comparison is seen. The FE trough is always wider than the empirical trough which is consistent with results published in the literature (e.g. Addenbrooke et al.,1997).

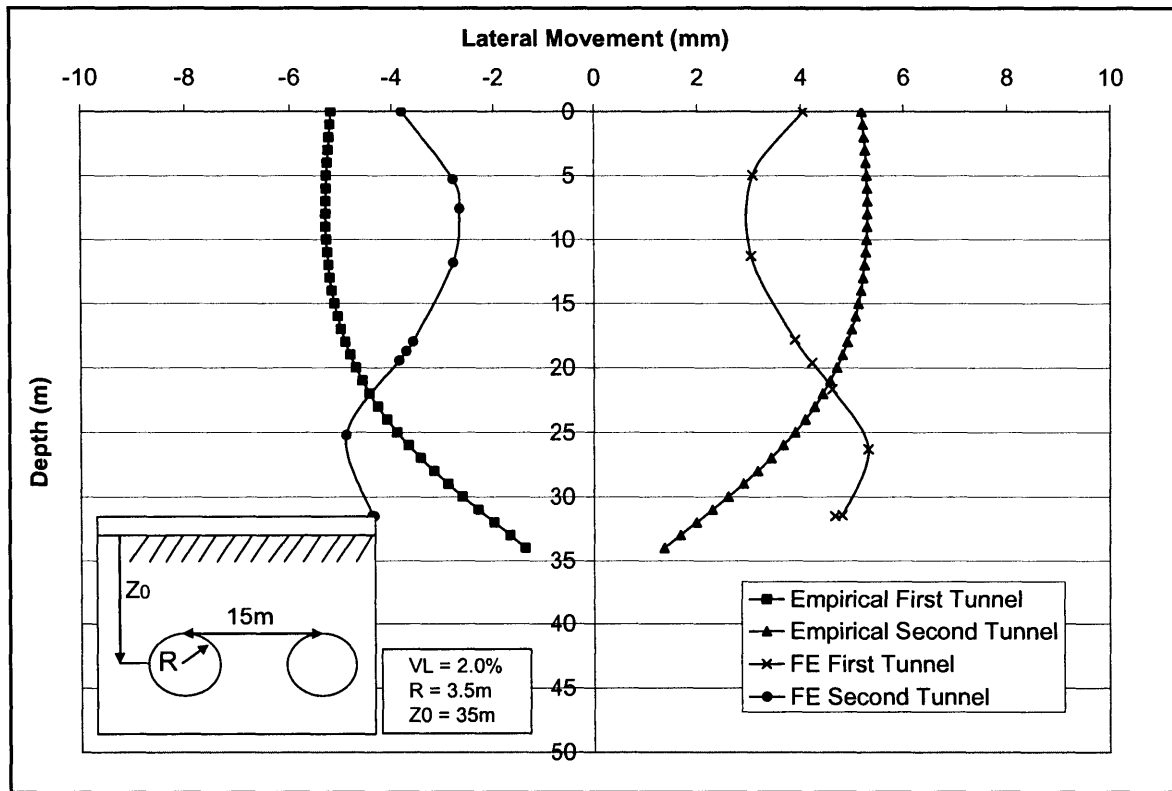


Figure 38. FE vs. Empirical lateral movements for side-by-side tunnels

Figure 38 compares the subsurface lateral movements estimated above each tunnel are compared. In this case both methods produce similar magnitudes of lateral deflection but differ in the vertical distribution of the movements.

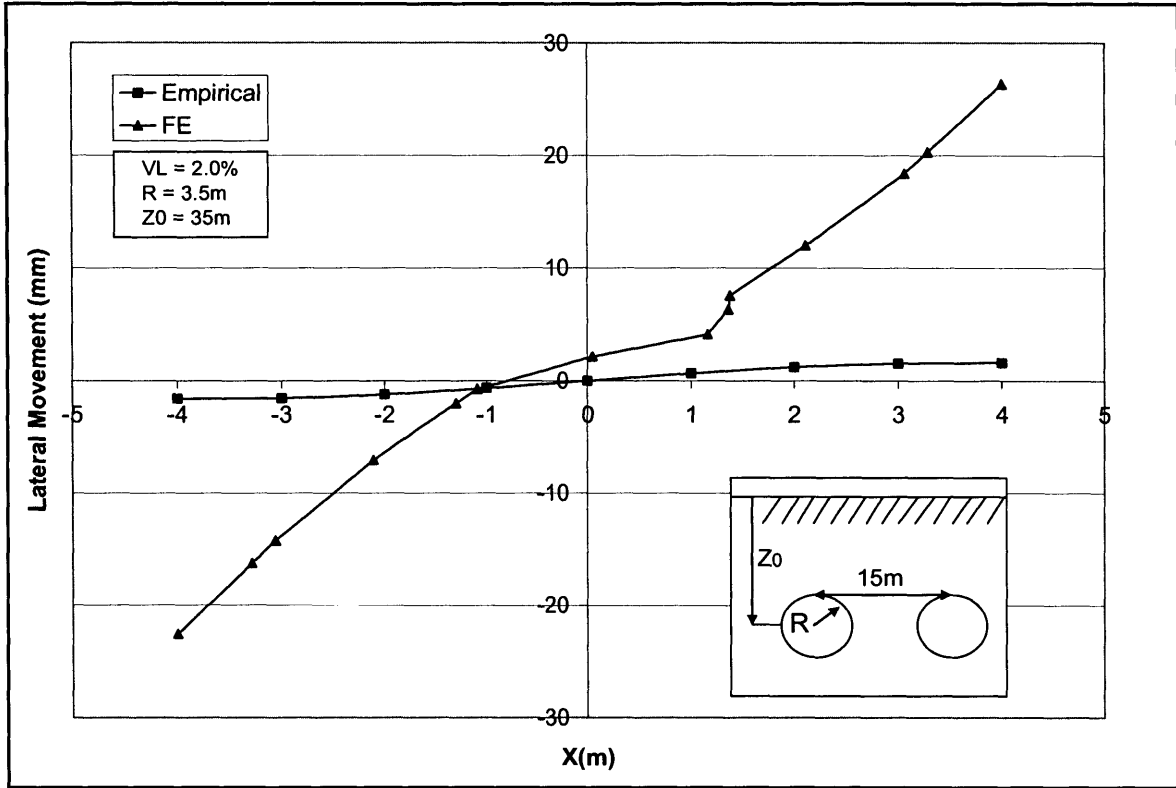


Figure 39. FE vs. Empirical lateral movements between side-by-side tunnels

Figure 39 shows the comparison of lateral movements in the zone directly between the two tunnels. There is a huge difference, with empirical methods estimating 1-2mm of net lateral movement, while finite element estimates 30mm. However, both methods estimate a net movement of zero at the mid-point between the tunnels. The plastic zone, which is located at a 3.5m zone surrounding the tunnel, is the cause for the large difference, as the two plastic zones are so close to each other. For the lateral deformations the finite element analysis computes a much larger lateral movement than the empirical methods.

5.1.2 Piggyback Tunnels

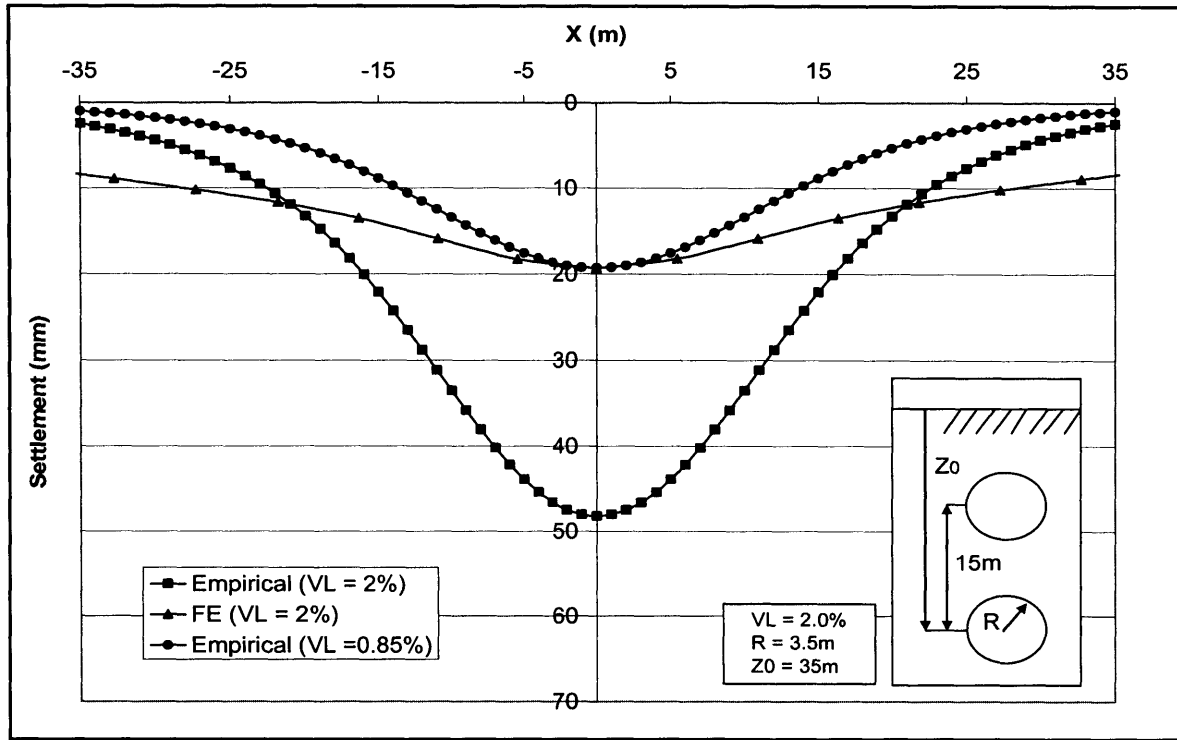


Figure 40. FE vs. Empirical surface settlement troughs for piggyback tunnels

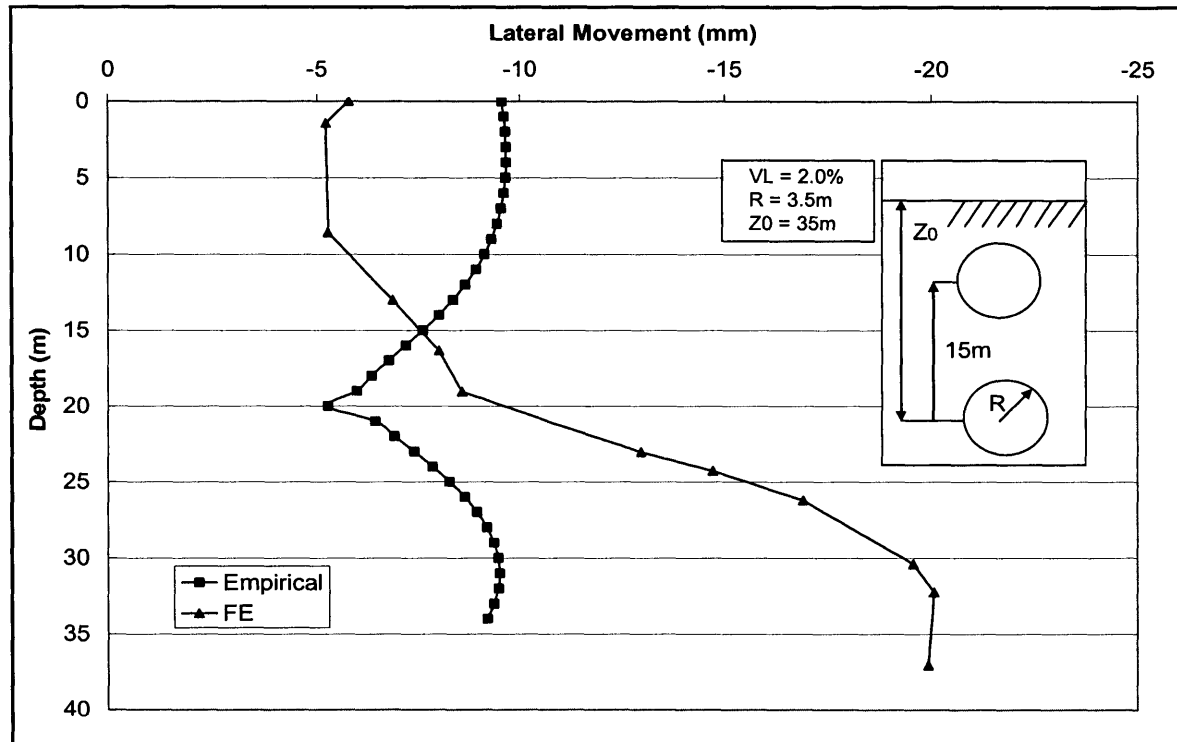


Figure 41. FE vs. Empirical lateral movements for piggyback tunnels

Figures 40 and 41 show the comparison for surface and subsurface movements for piggyback tunnels (lower tunnel constructed first), respectively. The surface settlement profile shows a huge difference in maximum settlement, 19mm for the finite element and 48mm for the empirical. The indirect comparison, using a $V_L = 0/85\%$ shows that even if the maximum settlements are the same that the Finite element trough is wider.

The lateral movements, in Figure 41, are estimated at a distance of 10m from the tunnel centerlines. The empirical methods estimate a larger deformation above the upper tunnel with minimum deflection at the springline of the upper tunnel ($S_x \approx 5\text{mm}$). In contrast the FE analyses show larger lateral deflections around the lower tunnel ($S_x \approx 20\text{mm}$ at the springline).

5.1.3 Angular-Offset Tunnels

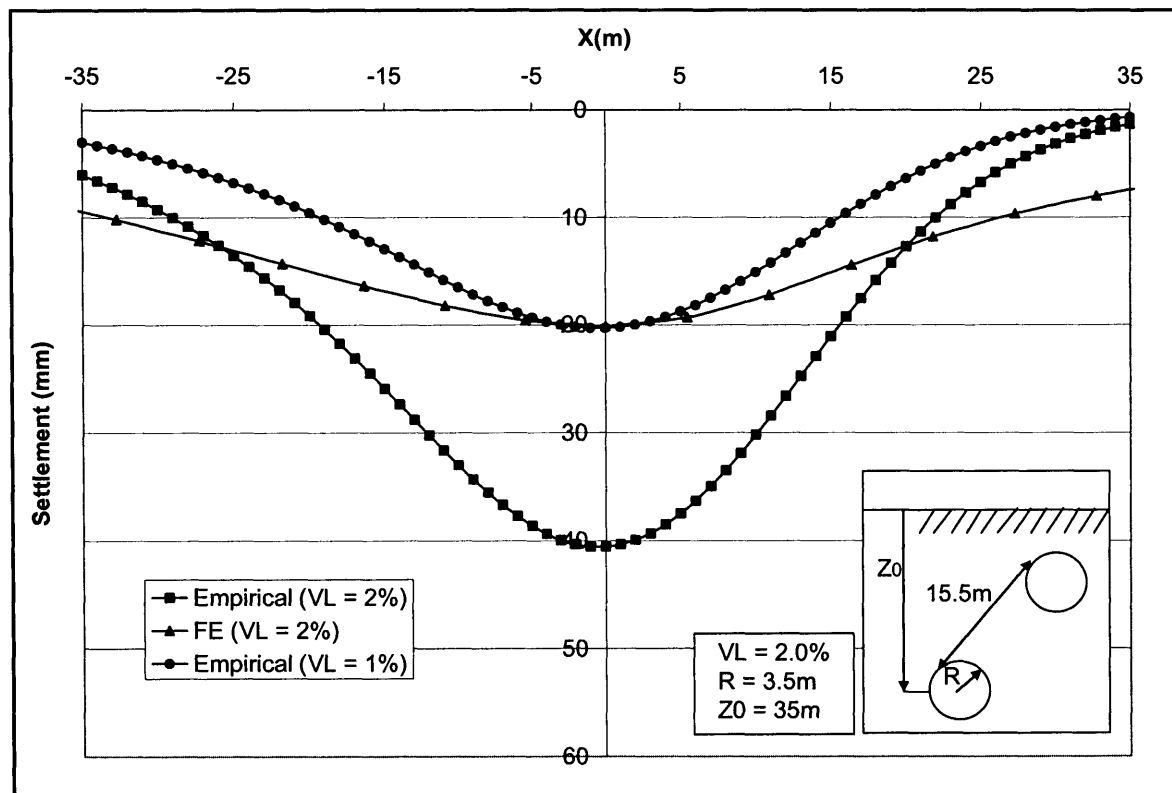


Figure 42. FE vs. Empirical surface settlement troughs for angular tunnels

Figure 42 shows the settlement troughs for 45 angular-offset tunnels spaced at 15.5m (lower tunnel constructed first). As in the previous comparisons, the maximum settlement for the empirical analysis is higher than the finite element estimate. In this situation, the estimate is double, being 20mm and 40mm respectively. The finite element trough is much wider than the empirical trough. Using $V_L = 1\%$, the finite element trough is again shown to be wider.

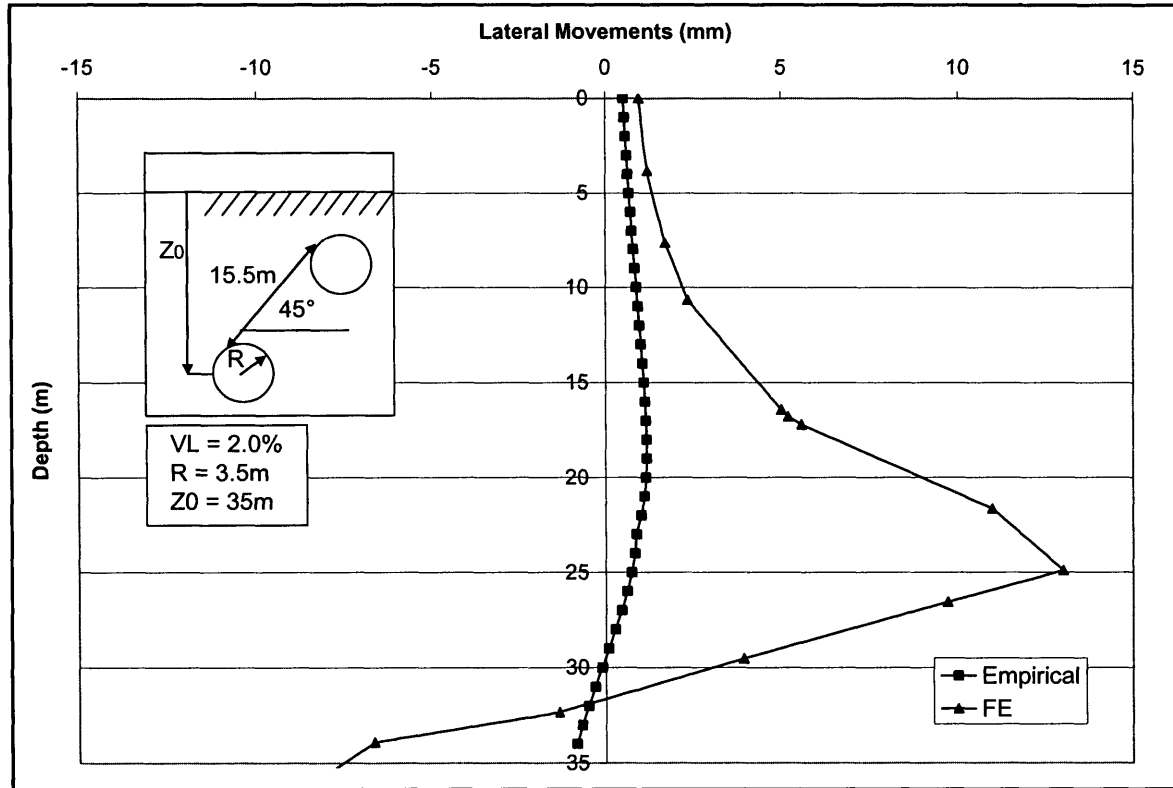


Figure 43. FE vs. Empirical lateral deformations for angular tunnels

Figure 43 shows the estimated lateral movements for 45° angular-offset tunnels, taken at the midpoint between the two tunnels. The net movements for the empirical methods are very low (0mm-1mm). The finite element curve shows a maximum deformation of 13mm. The reason for this is related to the plastic zone that is in close proximity to the midpoint of the tunnels. The elastic theory used in empirical methods does not take this into account though the basic shape of each method is very similar.

6.0 CONCLUSIONS

This thesis has outlined and applied the methods used to analyze the effects of twin tunnel construction. Empirical methods, derived from data recorded almost exclusively from single tunnel situations. In order to apply these methods to twin tunnel situations, the principle of superposition is applied. The other method is using non-linear finite element analyses, which can be used to calculate ground movements and lining stresses.

Empirical estimates of the surface settlements are based on Gaussian distribution functions. These results show that the piggyback tunnel configuration generates the highest gradient of surface settlements. Empirical equations for subsurface settlement profiles generally give settlement increasing with depth.

The forces that were calculated in the tunnel lining were calculated using Plaxis. As, expected, in side-by-side tunnels the bending moment is larger the closer together the tunnels are. With piggyback tunnels, the order of construction is very relevant to determine the distribution of the bending moment in each tunnel. If the upper tunnel is built after the lower tunnel, the bending moment in the lower tunnel's lining reduces significantly. The best solution for this is to construct the upper tunnel first, which will reduce the maximum bending moment in the system. For angular tunnels the order of construction has no consequence on the bending moment distribution.

The final part is the comparison of the two methods. For the surface settlement troughs, the shape was very similar but the empirical methods gave a larger maximum settlement and narrower troughs. For the lateral deformations, there were very little similarities with shape, although sometimes the magnitude was quite close. It was clear that empirical methods and finite element methods are not directly comparable.

REFERENCES

- Addenbrooke T.I., & Potts, D.M., 2003, "Twin Tunnel Interaction: Surface and Subsurface effects", Imperial College, London.
- Addenbrooke, T., Potts, D.M. and Puzrin A.M. (1997), "The influence of pre-failure soil stiffness on the numerical analysis of tunneling", *Geotechnique*, Vol. 47, No. 3, pp. 693-712.
- Attewel, P.B, Yeates, J & Selby, A.R., 1986, "Soil Movements induced by tunneling and their effects on pipelines and structures", Blackie.
- Institute of Civil Engineers, 2004, "Tunnel Lining Design Guide" Thomas Telford. London, The British Tunneling Society.
- Loganathan, N. & Flanagan, R.F., 2001, "Predictions of tunneling induced ground movements: Assessment and evaluation" *Underground Singapore 2001*, pp. 102-113.
- Mair, R.J., Taylor, R.N., 1993. "Prediction of Ground Movements and Assessment of Risk to Building Damage due to Bored Tunneling", *Geotechnical Aspects of Tunneling in Soft Ground*, Rotterdam, Balkema, pp. 713-718, 1996.
- MFISH, 2006, "Subway Remediation at Nicoll Highway Station", M.Eng Design Project, Massachusetts Institute of Technology.
- Møller, PhD, U. Stuttgart, 2006 Chapter 2, "Modern Tunneling Methods" pages 11-19, Chapter 3, "Classical Design Methods for Tunnels" pp. 32.
- O' Reilly, M. P., Mair, R.J., & Alderman, G.H., 1991, "Long term settlement over tunnels: an eleven year study at Grimsby" *Proceedings of Tunneling Symposium*, London.
- O'Reilly, M.P. & New, B.M., 1982, "Settlements above tunnels in the United Kingdom, their magnitude and prediction", *Tunneling London*.
- Peck, R. B., 1969. "Deep Excavation and Tunneling in Soft Ground", *Proceedings of the 7th International Conference of Soil Mechanics*, Mexico, State-of-art Volume, pp. 225-290.
- Peck, R.B, Hendron, A.J., & Mohraz B., 1972, "State of the Art Soft-Ground Tunneling", *Proceedings of the Rapid Excavation and Tunneling Conference*, Chicago, IL, Vol 1.
- Whittle, A.J. & Sagaseta, C., 2001, "Analyzing the Effects of Gaining and Losing Ground", from 'Soil Behavior & Soft Ground Construction' *ASCE GSP 119*, pp. 225-290.